Yepes, V.; García Segura, T.; Moreno-Jiménez, J. (2015). A cognitive approach for the multi-objective optimization of RC structural problems. Archives of Civil and Mechanical Engineering. 15(4):1024-1036. doi:10.1016/j.acme.2015.05.001.

A cognitive approach for the multi-objective optimization of RC structural problems

V. Yepes[1]

T. García-Segura[2]

J.M. Moreno-Jiménez[3]

Abstract

This paper proposes a cognitive approach for analyzing and reducing the Pareto optimal set for multi-objective optimization (MOO) of structural problems by means of jointly incorporating subjective and objective aspects. The approach provides improved knowledge on the decision-making process and makes it possible for the actors involved in the resolution process and its integrated systems to learn from the experience. The methodology consists of four steps: (i) the construction of the Pareto set using MOO models; (ii) the filtering of the Pareto set by compromise programming methods; (iii) the selection of the preferred solutions, utilizing the relative importance of criteria and the Analytic Hierarchy Process (AHP); (iv) the extraction of the relevant knowledge derived from the resolution process. A case study on the reinforced concrete (RC) I-beam has been included to illustrate the methodology. The compromise solutions are obtained through the objectives of economic feasibility, structural safety, and environmental sustainability criteria. The approach further identifies the patterns of behavior and critical points of the resolution process which reflect the relevant knowledge derived from the cognitive perspective. Results indicated that the solutions selected increased the number of years of service life. The procedure produced durable and ecological structures without price trade-offs.

Keywords

Multi-objective optimization; Analytic Hierarchy Process; reinforced concrete structures; ecological and economic sustainability; cognitive decision making.

[1] Associate Professor, Institute of Concrete Science and Technology (ICITECH), *Universitat Politècnica de València*, 46022 Valencia, Spain. **Corresponding author**. Phone +34963879563; Fax: +34963877569; E-mail: vyepesp@upv.es

[2] Graduate Research Assistant, Institute of Concrete Science and Technology (ICITECH), *Universitat Politècnica de València*, 46022 Valencia, Spain. E-mail: tagarse@cam.upv.es

[3] Professor, Grupo Decisión Multicriterio Zaragoza (GDMZ). Universidad de Zaragoza. Zaragoza, Spain. E-mail: moreno@unizar.es

1 Introduction

Quality, constructability, safety, and cost are conflict aspects that are usually considered in the planning and design of a project. Decisions made in such complex contexts require the development of new decisional tools and methods that provide more effective and realistic solutions [1,2]. Achieving a compromise solution from a cognitive perspective oriented to learning about the decision making process and educating the actors involved in the resolution process [3–5] is the main target for a cognitive multi-objective optimization (MOO) model in the Knowledge Society.

Metaheuristics have been used as an MOO technique in construction projects [6]. Chiu and Lin [7] maximized the maintenance strategies and minimized the life cycle cost, the failure probability, the cracking probability of concrete covers, and the maintenance times of RC buildings. Paya et al. [8] optimized RC building frames in terms of constructability, economic cost, environmental impact, and overall safety. Martinez-Martin et al. [9] minimized the economic cost, the reinforcing steel congestion, and the CO_2 emissions of an RC bridge pier. The present study suggests that service life should be a criterion for dealing with structural decay from the design phase. The carbonation phenomenon is addressed from the perspective of RC decay and carbon capture [10–12].

On the other hand, MOO problems can be categorized in accordance with how the decision-maker (DM) articulates preferences. In this context, the use of Pareto set does not require a previous articulation of preferences. Many methods have been created with the intent of abbreviating the set of Pareto solutions [13]. The “knee method” [14] is a *posteriori* method that identifies the points for which an improvement in one objective results in a significant worsening of at least one other objective. Clustering methods gather solutions in groups to later provide some representative solutions [15]. Filtering methods eliminate solutions that offer little information to the designer. The filter can be applied after the Pareto set formation [16].

The a-*posteriori* approach allows relevant knowledge to be obtained, since the decision making takes place after obtaining the multiple trade-off. However, the decision maker has to choose among a wide range of solutions. We address the gap between searching for multiple trade-off solutions, choosing preferred solutions and obtaining useful knowledge, by combining heuristic optimization with AHP. AHP has been integrated with many heuristic/meta-heuristic approaches to solve production planning problems [17]. Instead, little attention has been paid to the structural design context.

We propose a *posteriori* systematic procedure that filters the Pareto frontier, presents an easy technique to choose preferred solutions, and simultaneously provides relevant knowledge derived from the resolution process. The cognitive orientation of this approach is based on the exploitation of the mathematical model used for the multi-objective optimization of RC structural problems from a learning perspective. The mission is not only concerned with selecting a product (RC I-beam) but with extracting information that improves the existing knowledge about the decision making process and, finally, with educating the actors involved in the resolution of the problem. This 3P (Product, Process and Person) orientation [18] permits to deal with the new needs and challenges of the Knowledge Society, in particular the integration into the formal models of the objective aspects associated with the traditional scientific method with the subjective ones associated with the human factor [19].

This methodology is tested in a structural application to find a sustainable balance between the economic cost, the CO_2 emissions and the service life of a high-strength RC I-beam. The cognitive orientation of this particular case provides valuable knowledge oriented toward achieving a sustainable structural design with the aim of educating the actors in this approach.

2 Preferred solutions in Pareto Sets $[PS]^2$ for multi-objective optimization problems

This paper proposes a four-step methodology for identifying the preferred solutions for the DM in Pareto sets (see Figure 1). In the first step, MOO leads to a range of optimal solutions termed the Pareto set of solutions. The second step reduces the number of Pareto points using the closest solutions to the ideal, according to three Minkowsky metrics (Figure 2). We propose a filter that selects the closest solution to the ideal point according to random Analytic Hierarchy Process (AHP) [20] pairwise comparison matrices, which guarantee good consistency.

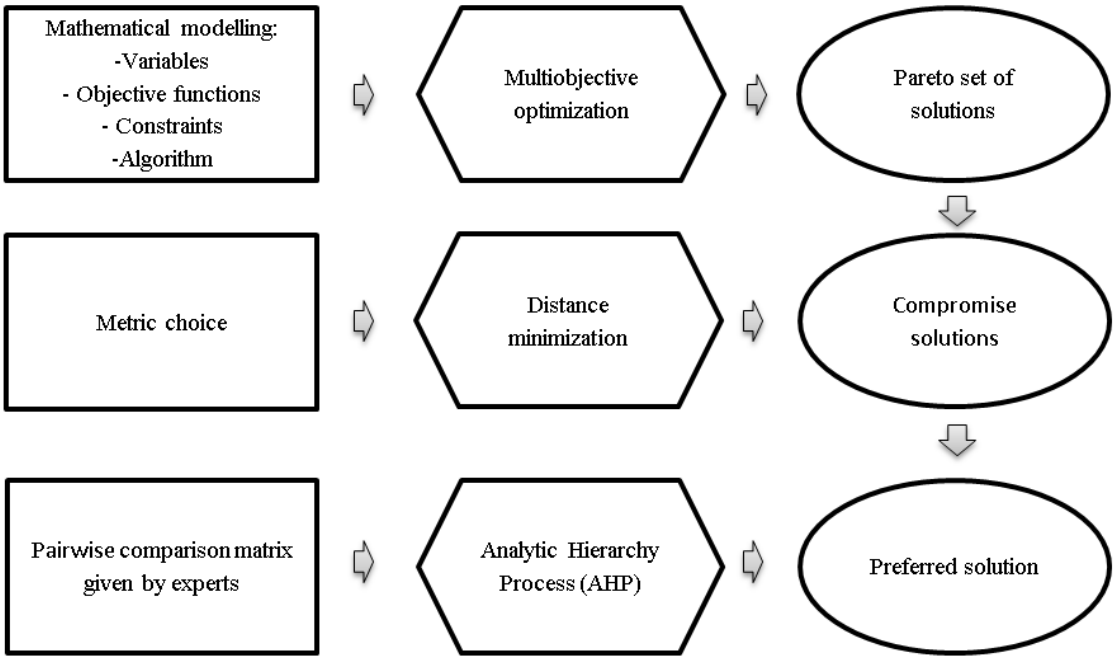

Figure 1. $[PS]^2$-methodology

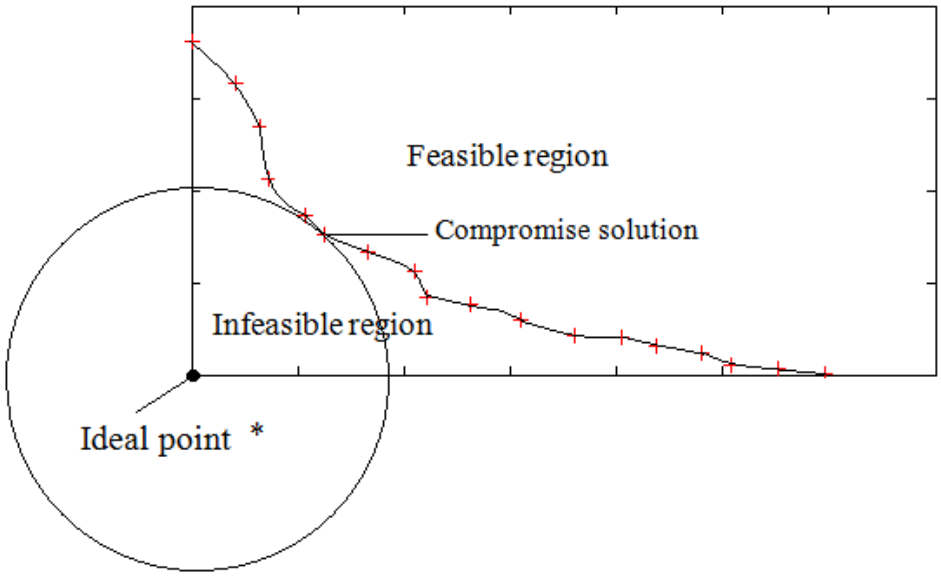

Figure 2. Compromise solution using the L_2 norm

The three metrics of the Minkowski family used for filtering the Pareto set are the Manhattan (L_1), Euclidean (L_2) and Tchebycheff (L_∞). The distance from any point $z(x) \in Z \subset R^q$ to the ideal vector is evaluated in the p norm by (1):

$$L_p = d(z(x), z^*, p) = [\sum_{j=1}^{q} \lambda_j^p \left| z_j^* - z_j(x) \right|^p]^{1/p} \qquad p=1,2\ldots$$

$$L_\infty = \lim_{p\to\infty} L_p = \max_{j=1,\ldots,q} \lambda_j \left| z_j^* - z_j(x) \right| \quad (1)$$

Note that $z_j(x)$, $j = 1, \ldots, q$ are the criteria addressed in the problem that, without prejudice to the generality, are supposed to be maximized, $z^* = (z_1^*, \ldots, z_q^*)$ is the ideal vector, and λ_j ($j = 1, \ldots, q$) are the weights associated with the criteria (2). These weights are composed of a subjective component (w_j), which incorporates the relative importance of each criterion, and an objective component (δ_j) to normalize the values associated with the criteria. The criteria priorities (w_j) are obtained through the AHP pairwise comparison matrices [20]. The expert priorities are randomly selected in the second stage (Section 3.2).

$$\lambda_j = w_j / \delta_j = \frac{w_j}{\max_{x\epsilon X} |z_j(x)|} \quad (2)$$

The third step involves choosing the preferred solution according to the DM's preferences. The priorities are provided by a set of experts (Section 3.3). We use the AHP to derive the subjective components of the criteria priorities or weights. Finally, the fourth stage uses a cognitive approach to extract the relevant knowledge derived from the resolution process.

3 Case study

3.1 Step 1: Multi-objective optimization

3.1.1 Mathematical modeling

The problem outlined by this paper consists in designing a RC I-beam which involves the optimization of three objective functions and the simultaneous checking of constraints g_i imposed by design codes. Eq. (3), Eq. (4) and Eq. (6) evaluate the objective functions for the economic cost (C), the CO_2 emissions (E), and the service life (SL).

$$C(x) = \sum_{i\epsilon Ic} p_i . m_i(x) \quad (3)$$

where p_i are the unit prices and m_i are the measurements. The indices set (Ic) of structural costs includes concrete, steel, formwork, placing, and CO_2 costs.

$$E(x) = \sum_{i\epsilon Ie} e_i . m_i(x) - C_{co2}(x) \quad (4)$$

Note that e_i is equal to the unit emissions, C_{CO2} is the kilograms of CO_2 captured by the concrete surface (5), and Ie is the indices set contributing to the structural emissions. The CO_2 capture was evaluated according to Equation (5) by García-Segura et al. [21] based on the predictive models of Fick's First Law of Diffusion and the study of Lagerblad [22] and Collins [11].

$$C_{co2}(x) = k(x) \cdot \sqrt{SL(x)} \cdot c(x) \cdot CaO \cdot pc \cdot A(x) \cdot M \quad (5)$$

with the carbonation rate coefficient, $k(x)$, depending on the variable concrete strength; the years of the structure service life (SL(x)); the quantity of Portland cement per cubic meter of concrete ($c(x)$); the CaO content in Portland cement (CaO = 0.65); the proportion of calcium oxide that can be carbonated (pc = 0.75); the exposed surface area of concrete ($A(x)$), which is conditioned by the geometric variables; and the chemical molar fraction CO_2/CaO (M = 0.79). Eq. (6) evaluates the service life:

$$SL(x) = \left(\frac{r(x)}{k(x)}\right)^2 + \frac{80 \cdot r(x)}{\emptyset_r(x) \cdot v_c} \quad (6)$$

where r is the variable concrete cover (mm), k is the carbonation rate coefficient (mm/year$^{0.5}$), $\emptyset_r$ is the most restrictive variable for the bar diameter (mm), and v_c is the corrosion speed (μm/year).

The I_G weak constraints are given by Eq. (7), and include those required to guarantee the structural safety and constructability.

$$\mathrm{G_i(x)} + n_i - p_i = \hat{G}_i, \ \mathrm{i} = 1, \dots, I_G \quad (7)$$

Finally, the feasible set (hard constraints) for the designer variables is given by Eq. (8):

$$X = \{\mathrm{x} \in R^n | \mathrm{g_i(x)} \leq 0, \mathrm{i} = 1, \dots, \mathrm{m}\} \quad (8)$$

3.1.2 Variables and parameters

The RC I-beam is defined by 20 discrete design variables (Figure 3). The geometry is defined by the depth (h), the width of the top flange (b_{fs}), the width of the bottom flange (b_{fi}), the thickness of the top flange (t_{fs}), the thickness of the bottom flange (t_{fi}), the web thickness (t_w), and the concrete cover (r). Reinforcing bars are defined by the number of bars (n_1, n_2, n_3) or the number of bars per meter (n_4, n_5) and the diameter ($\emptyset_1$, $\emptyset_2$, $\emptyset_3$, $\emptyset_4$, $\emptyset_5$, $\emptyset_6$, $\emptyset_7$). The design distinguishes the transverse diameter in the supports and the midspan (3L/5). The lower reinforcement is divided into two systems, one covering the whole beam length (n_2, $\emptyset_2$) and another covering the midspan (n_3, $\emptyset_3$). Finally, the last variable describes the concrete compressive strength (f_{ck}), which varies between 30 and 100 MPa. This structure was also proposed by García-Segura et al. [21] to optimize self-compacting concrete. The parameters are the permanent distributed load (20 kN/m), the variable distributed load (10 kN/m), the beam span (15 m), the exposure class (IIb), the percentage of occluded air (< 4.5%), and the use of Portland CEM.

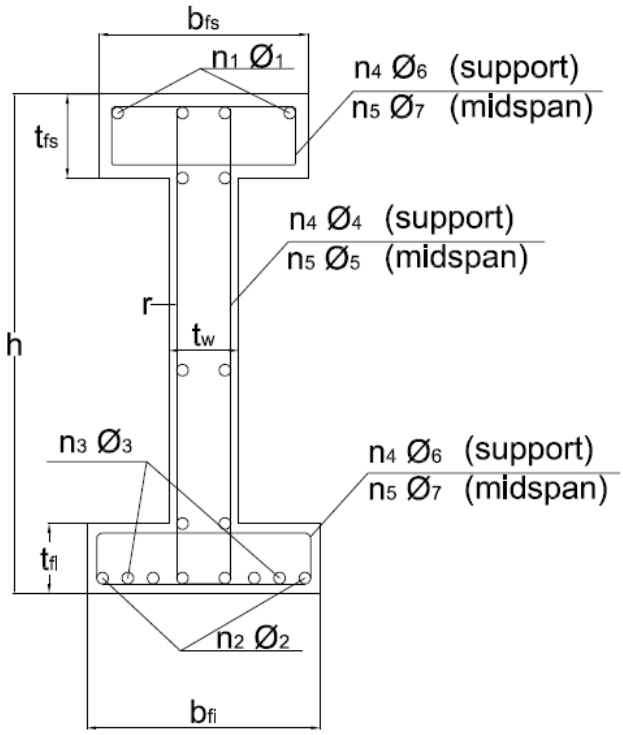

Figure 3: Design variables of the reinforced concrete I-beam

3.1.3 Objective functions

The total cost is the result of the construction unit costs involved in RC production and placement. Added to this are the CO_2 cost established by the European Union Emission Trading Scheme [23]. The CO_2 emissions are the result of all material production and transport, as well as the emissions derived from the energy used for the beam placing. The unit prices p_i and unit emissions e_i (see Table 1) were obtained from the BEDEC ITEC database [24], with the exception of the plasticizer emission, which was obtained from the European Federation of Concrete Admixtures Associations [25], and the silica fume, which was considered not to produce emissions due to its waste origin.

Carbonation is the main factor leading to RC decay when the structure experiences general exposure. At the same time, the carbonation absorbs CO_2 and therefore this capture is deducted from the emissions. The amount of CO_2 captured during the service life is assessed according to Eq. (5). The carbonation rate coefficient and the quantity of Portland cement per cubic meter of concrete are given in Table 2.

The service life (6) is characterized by the number of years that the RC structure is capable of lasting according to the physical and chemical conditions to which it is exposed. The Spanish Concrete Code [26] considers that service life is the sum of the initiation of corrosion and its propagation [27]. The

maximization of this objective depends on the concrete used, the concrete cover, and the diameter of the reinforcing bars. All of these are part of the design variables. The corrosion speed has a value of 2 μm/year in exposure class IIb [26].

3.1.4 Constraints

The weak constraints (7) represent the serviceability and ultimate limit states (SLS and ULS) imposed by the Spanish Code [26] for this structure. The hard constraints (8) are the permissible set of values that can be adopted by the variables. The global analysis of the structure was carried out in accordance with a linear analysis methodology. The SLS for cracking does not allow the crack width to exceed 0.3 mm. The instantaneous and time-dependent deflection of the central section is limited to 1/250 of the beam span. The ULS checks the flexure and shear limit state. The ULS of flexure calculates the ultimate iteration diagram *Nu–Mu* and then checks whether the acting bending resultant M_d is in the diagram. The shear limit state is verified similarly, as the ultimate force is greater or equal to the design load effect. In addition, the minimum amount of reinforcement for stress requirements and the geometrical conditions are also examined. Durability conditions demand a service life of 100 years; this is calculated by Eq. (6).

3.1.5 Algorithm

Multi-Objective Simulated Annealing (MOSA) has been widely used since Serafini [28] proposed it. Single-objective Simulated Annealing (SA) simulates the crystal formation process and is the basis of the multi-objective optimization. The temperature controls the mobility, so that at high temperatures the possibilities for movement are large. Thanks to this property, the algorithm explores all around the search space during the first iterations in order to later focalize the search around better results. Metropolis et al. [29] established the probability of acquiring a thermal state proportional to exp (–Δ*E*/*T*). In contrast, Glauber [30] proposed a function that also rejects favorable solutions. Eqs. (9) and (10) show, respectively, the Metropolis and Glauber criteria. This paper studies both criteria to determine which is the most appropriate.

$$\text{random} < \prod_{i=1}^{i=3} e^{-\frac{f_{i,1}-f_{i,0}}{T_i}} \tag{9}$$

$$\text{random} < \prod_{i=1}^{i=3} \frac{1}{1+e^{\frac{f_{i,1}-f_{i,0}}{T_i}}} \tag{10}$$

where the meaning of the term $f_{i,t}$ is the value of the objective function i for the current solution (t=1) or the working solution (t=0), and T_i is the temperature associated to the objective function. Figure 4 shows the flowchart of the MOSA process. The initial temperature is calculated following Medina's method [31]. Once the temperatures for the three objectives are calibrated, a feasible solution is obtained. This solution is transformed by carrying out a small random variation of the 20% of the variables to a higher or lower value. The new solution is checked and evaluated. Then, the Pareto condition checks whether the solution is not shadowed by any Pareto solution. If it is a feasible solution and satisfies the Pareto condition, the solution is updated and included in the Pareto set of solutions. In case the solution complies with the Metropolis or Glauber criterion but not the Pareto condition, the solution is also updated even if it is not included in the Pareto front. This process is repeated until the temperature is lower than the initial temperature divided by 1,000,000 and there are no acceptances in 50 consecutive Markov chains. Note that the temperature decreases once a Markov chain ends ($T = \alpha T$) by means of a coefficient of cooling (α). To improve the search, the algorithm restarts every five chains from any of the solutions in the Pareto surface.

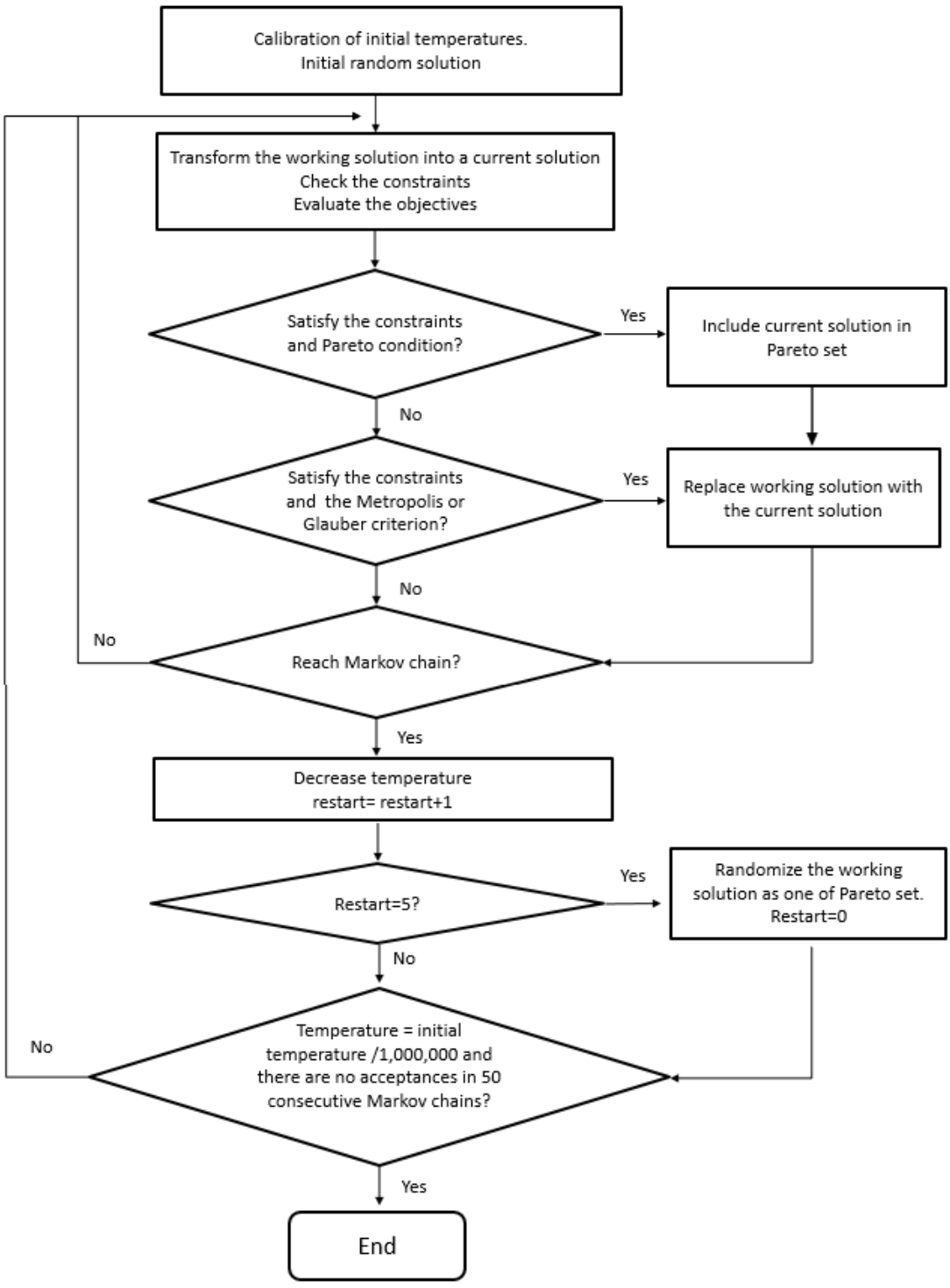

Figure 4: Flowchart of the MOSA process

3.1.6 Performance of the multi-objective model

The program was coded in Intel® Visual FORTRAN Compiler Integration for Microsoft Visual Studio 2010 with an INTEL® Core™ i7-3820 CPU processor with 3.6 GHz. In order to calibrate the algorithm parameters, several values have been used for the MOSA algorithm with the Metropolis and Glauber

criteria. The algorithm was executed 15 times to obtain the Pareto front. This ensures the solution quality for each objective according to the methodology proposed by Payá-Zarforteza et al. [32], based on the extreme value theory. The difference between the minimum cost and CO_2 emissions obtained from the 15 runs and the extreme value estimated using the three-parameter Weibull distribution that fits 2000 MOSA results is less than 0.99% and 0.62%, respectively. The best results for each algorithm and the algorithm parameters are summarized in Table 3.

The Metropolis criterion achieved the best results with Markov chains of 30,000 iterations and a cooling coefficient of 0.95. Using the Glauber criterion, better solutions in terms of cost and emissions were included in the Pareto set of solutions. That is because hard-to-find regions surrounded by few good solutions can be found by this algorithm thanks to the probability to reject better solutions. In this case, Markov chains of 10,000 iterations are recommended and a coefficient of cooling (α) of 0.95 (see Table 3). The solution is modified by a small random movement; 20% of the variables are modified by a higher or lower value. Therefore, Multi-Objective Simulated Annealing with Glauber criterion (MOSA-G) was chosen.

Figure 5 shows the Pareto set for the three objectives. The results are presented, highlighting the variable concrete strength. There was a clear trend towards increasing concrete strength and service life improvement. Indeed, a life of 500 years was only achieved by high-strength concrete. On the other hand, the emission reduction was influenced by the concrete strength for the same service life. The reduction in concrete strength led to better solutions in terms of CO_2 emissions but worse solutions from an economic point of view. It is worth noting that bigger cross-sections of low-strength concrete with a smaller amount of steel maximize the CO_2 capture and reduce the embedded emissions. The correlation between the emissions, the cost, the service life and the concrete strength is represented by a multiple linear regression (see Eq. (11)) with R^2= 0.87

$$\mathrm{E(kgCO_2)} = 6181.476 - 1.281 \cdot \mathrm{C(€)} + 4.916 \cdot \mathrm{fck(MPa)} + 0.196 \cdot \mathrm{SL(years)} \qquad (11)$$

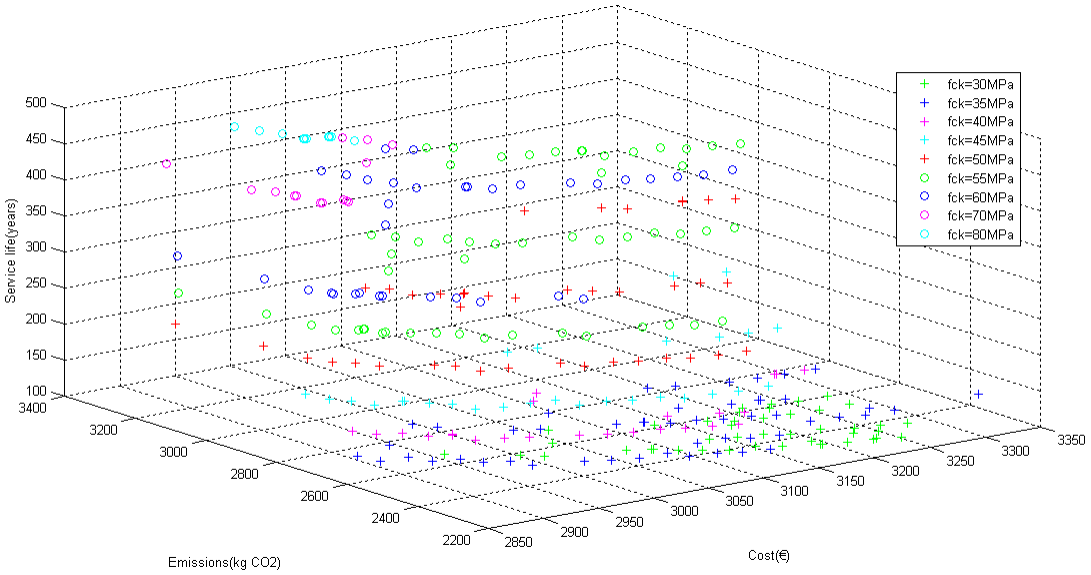

Figure 5: Pareto set of solutions

In the following, the Pareto set as ranges of service life (see Figure 6) is presented. Concrete from 30 to 45 MPa presented the best results for service lives between 100 and 200 years. If the service life rises to 300 years, concrete from 45 to 55 MPa should be chosen. Thereby, when we lengthen the service life to 400 years, 60 MPa concrete is also used. Finally, to achieve a service life of 400-500 years, concrete of 50-80 MPa is the best choice. Note that 90 and 100 MPa concretes are not Pareto solutions. Four parabolic fits may be used to describe the relationship between the cost (C) and the emissions (E) for service lives between 100 and 500 years (see Figure 6). The service life may be increased from 100 to 500 years by increasing the cost by 1% (obtained from the points (2895.48, 2713.78, 109.04) and (2912.15, 3115.03, 500)). Alternatively, the service life improvement involves a 10% increment in CO_2 emissions (obtained from the points (3242.66, 2258.91, 107.85) and (3169.70, 2486.74, 500)). Therefore, the findings indicated that durable structures can be designed without trade-offs in price or emissions.

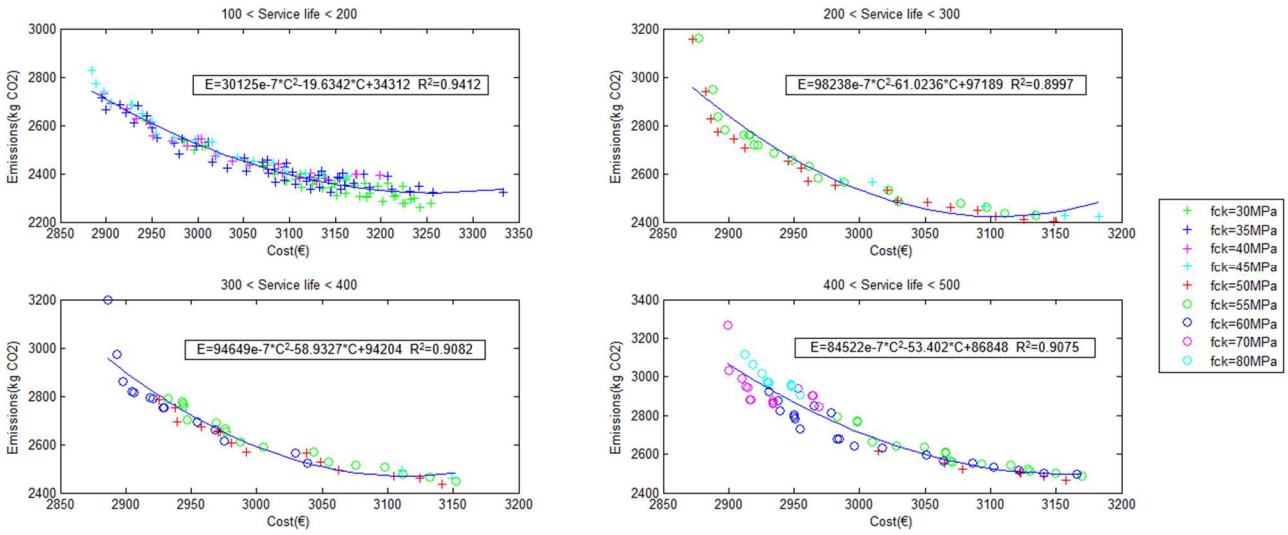

Figure 6: Pareto set according to service life range

3.2 Step 2: Distance minimization

In this step, the filter selected the closest solution to the point, according to random AHP pairwise comparison matrices. The consistency of the judgments was guaranteed and the sum of the weights provided by the matrix was always equal to one. The process reduced the Pareto set to a set of compromise solutions. This was undertaken for each metric (L_1, L_2, and L_∞). By analyzing the results, we reached conclusions under the influence of the DM and the metric used. Besides, the interpretation of the results provides knowledge regarding the characteristics of structural solutions which seek a good balance between criteria. In turn, the effect on the criteria values will show the contribution of each criterion to the ecological and economic sustainability.

Figures 7–18 show the best solutions for the metrics L_1, L_2, and L_∞ according to the criteria priorities. The vertices represent the points where the weight of the cost (S_1), the emissions (S_2) and the service life (S_3) are equal to one. The first three figures illustrate the concrete strength. Figure 7 shows the closest solutions when using the L_1 metric. In this case, only seven solutions from the 299-solution Pareto set resulted in compromise solutions. Therefore, the problem was drastically diminished. High-strength concrete (f_{ck} > 50 MPa) was used for any combination of weights. As the emission weight increased, the concrete strength decreased. Figures 8 and 9 display the results for the metrics L_2 and L_∞. The Euclidean metric reduced the problem to 18 solutions and the Tchebycheff metric expanded the possibilities to 46. Both revealed that the concrete with greater prospects for selection was 55 MPa concrete, since 50% of the compromise solutions used this grade of concrete. Figures 10–12 compare the cost results for the

metrics L_1 and L_∞. The findings indicated that L_1 and L_2 were more dependent on the criteria priorities. However, the variance of results decreased when using the L_∞ metric. The cost criterion was not severely affected by the improvement of other criteria. Therefore, compromise solutions presented a gradual cost variation influenced by the criteria priorities.

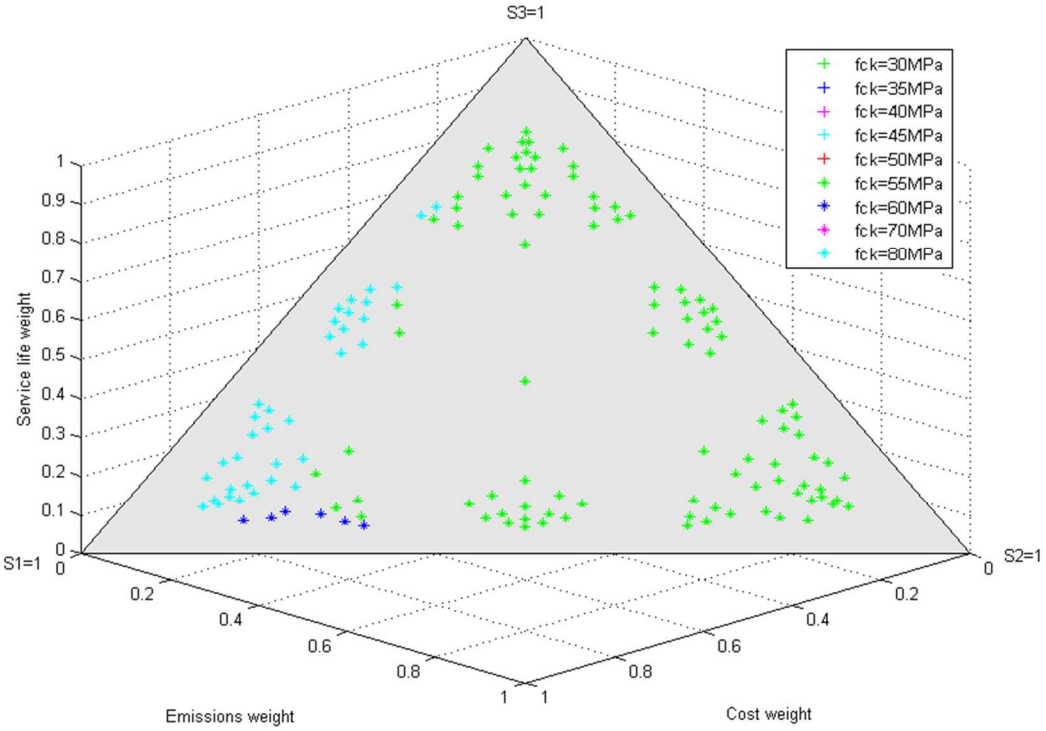

Figure 7: Compromise solutions according to the criteria priorities and L_1 metric. Results of concrete strength

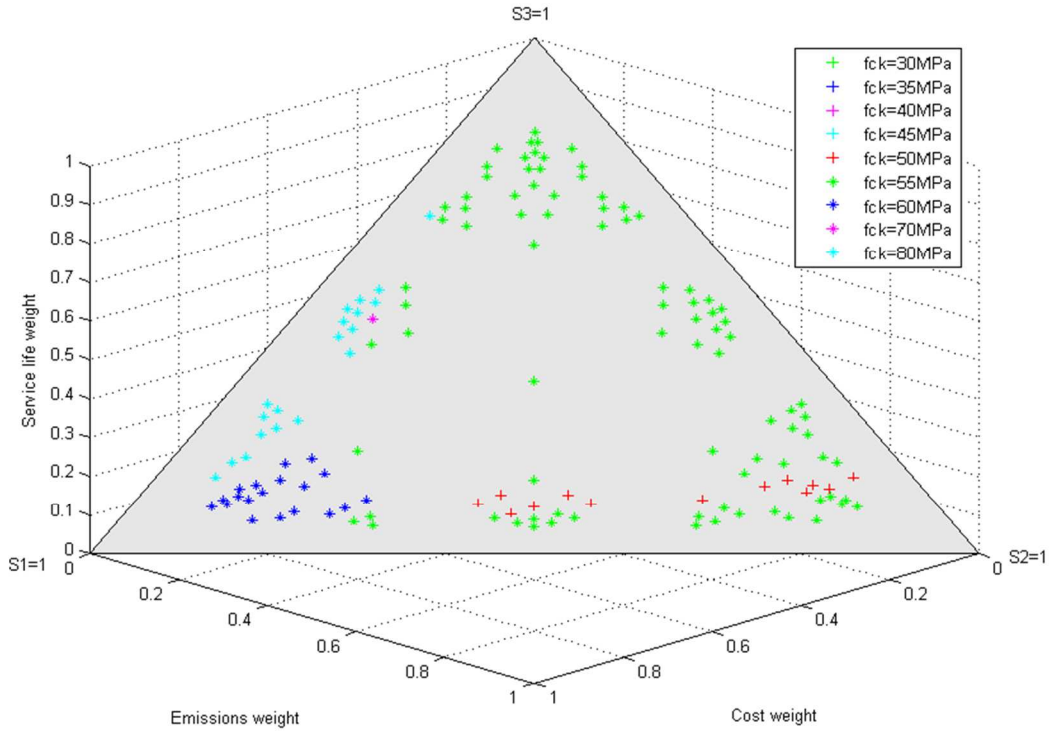

Figure 8: Compromise solutions according to the criteria priorities and L_2 metric. Results of concrete strength

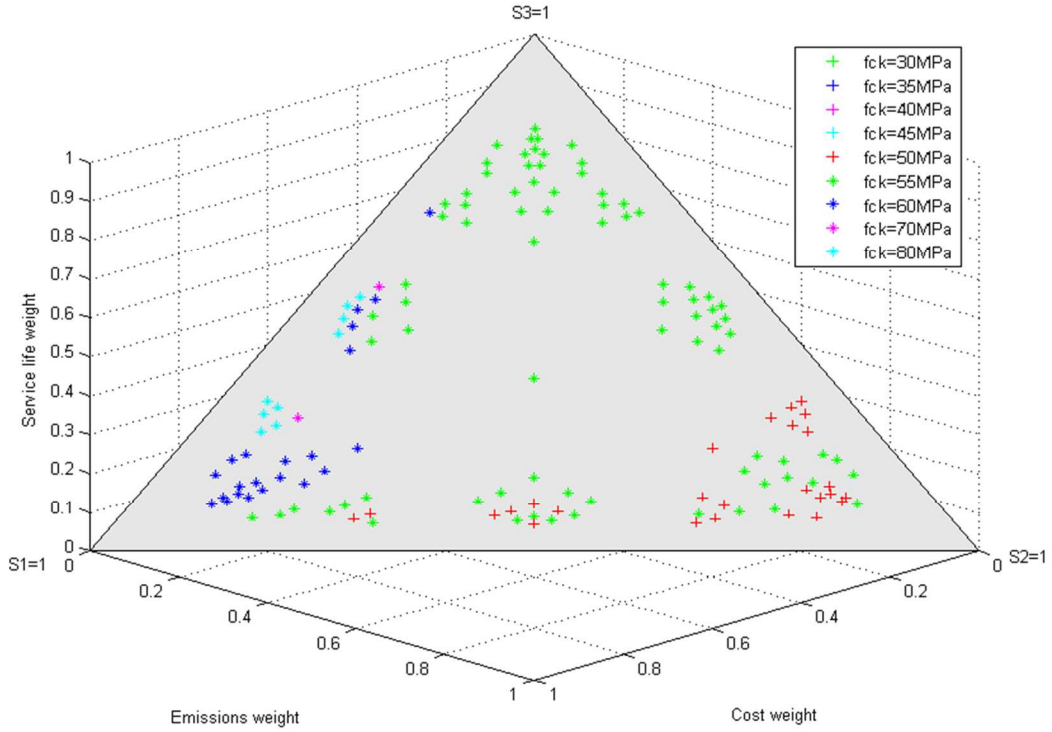

Figure 9: Compromise solutions according to the criteria priorities and L_∞ metric. Results of concrete strength

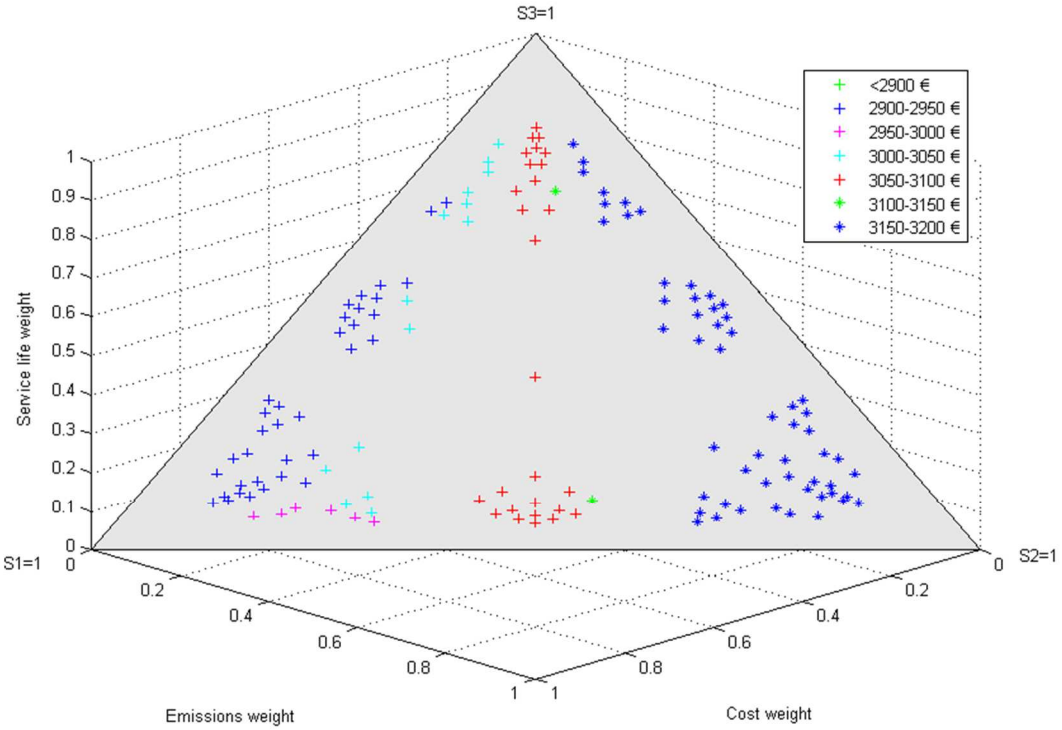

Figure 10: Compromise solutions according to the criteria priorities and L_1 metric. Results of cost

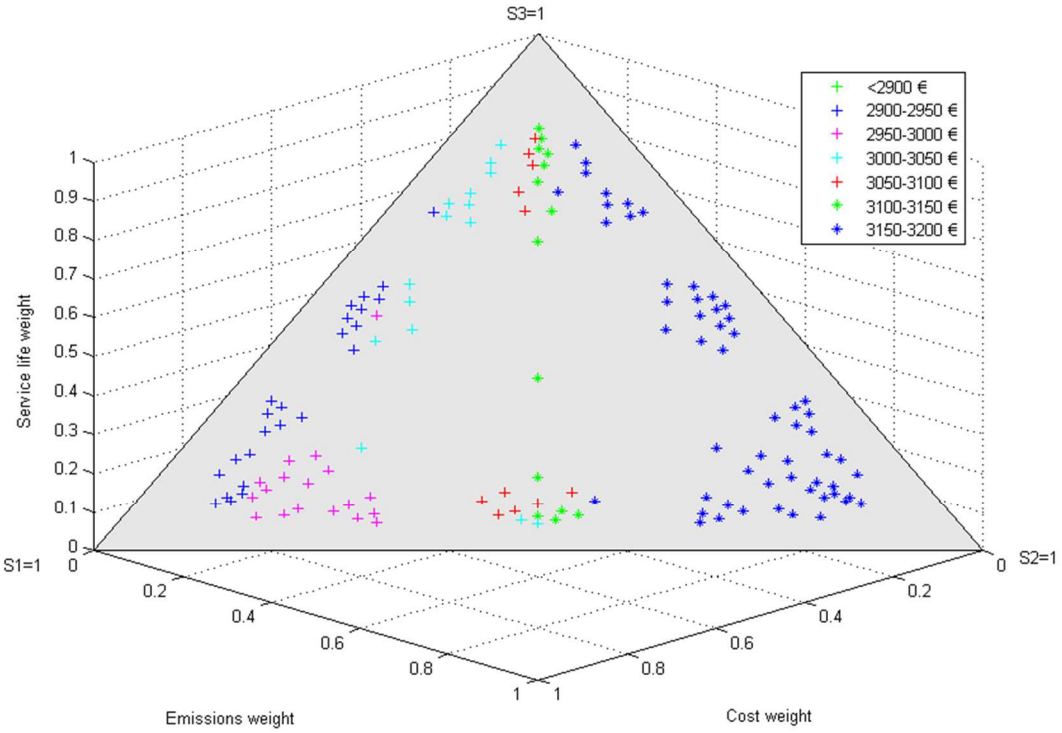

Figure 11: Compromise solutions according to the criteria priorities and L_2 metric. Results of cost

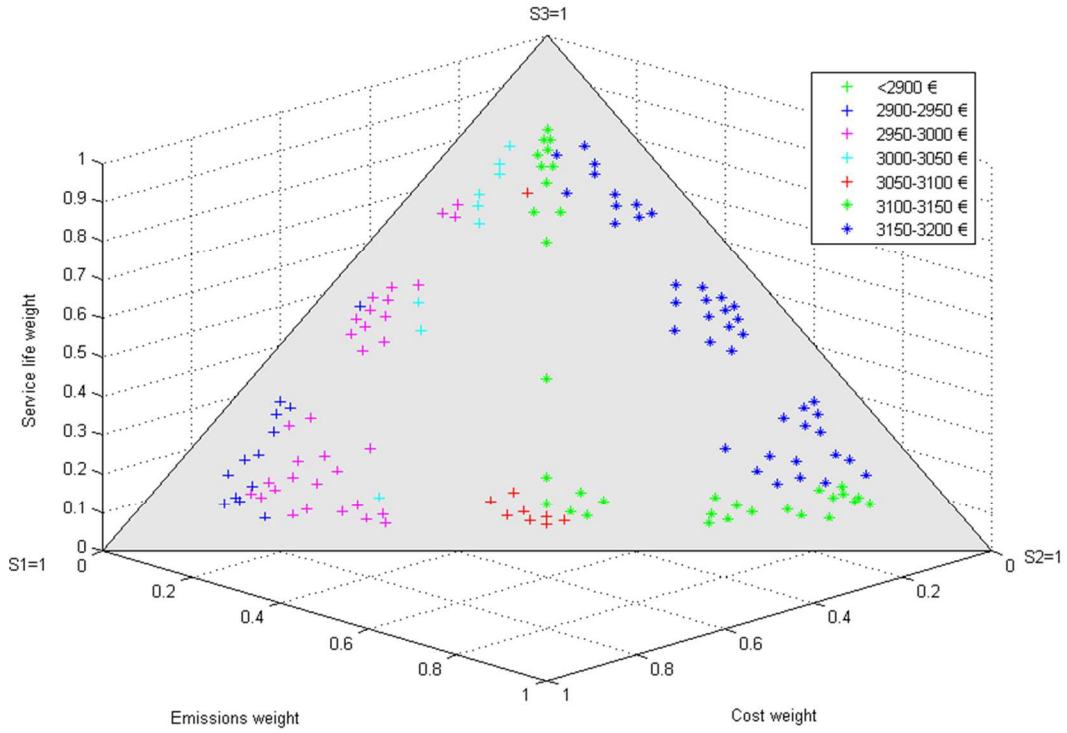

Figure 12: Compromise solutions according to the criteria priorities and L_∞ metric. Results of cost

Similar findings can be outlined when comparing the emissions (see Figures 13–15). The Tchebycheff metric found solutions with lower emissions. Likewise, more intermediate solutions (2700–2900 kg CO_2) were closer to the ideal solution using this metric. The most carbon-intensive solutions (3100–3200 kg CO_2) were only selected when the emission weight was near to zero and the metric was L_1. On the other hand, low-carbon solutions (2400–2600 kg CO_2) were chosen as long as the emission weight was greater than 0.3. The findings indicated that optimizing the emission criterion does not lead to a compromise solution, since the minimum emission solution was not included. However, small values of emissions that guarantee a long-term approach form the majority of the solutions.

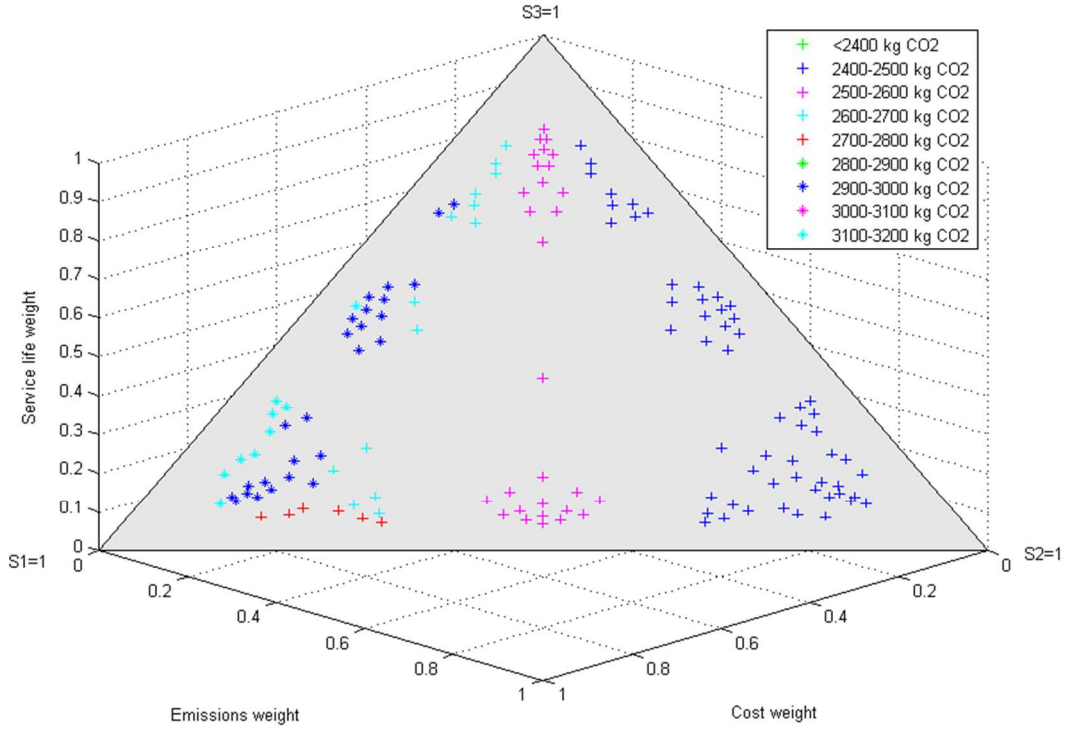

Figure 13: Compromise solutions according to the criteria priorities and L_1 metric. Results of CO_2 emissions

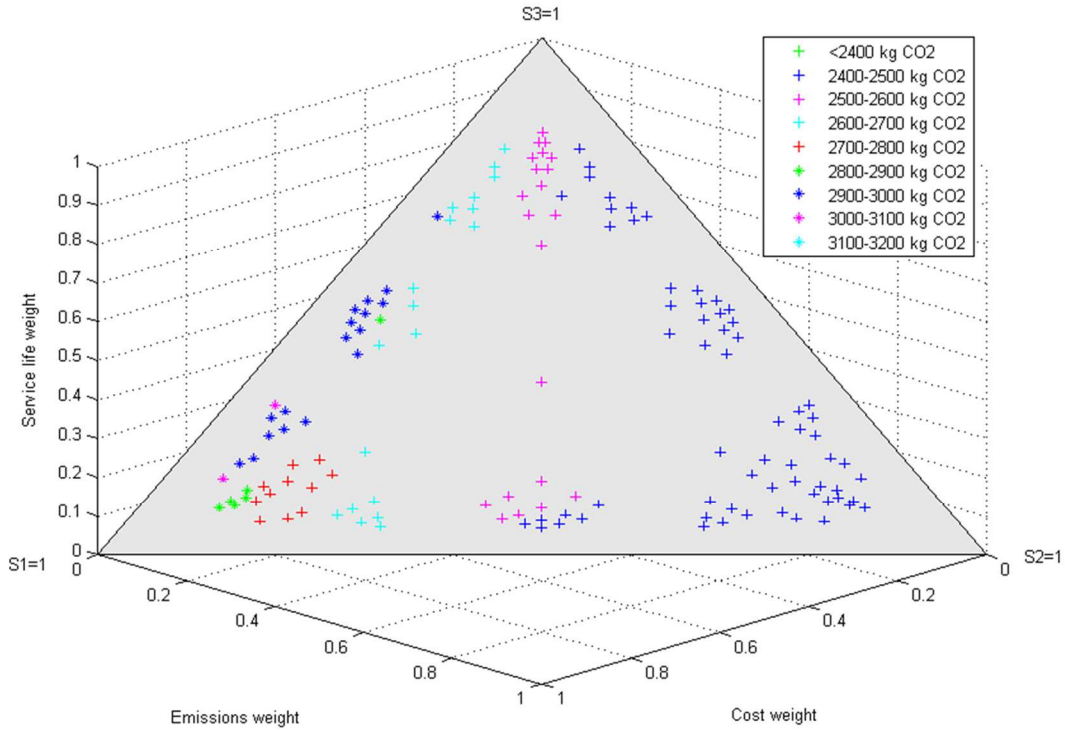

Figure 14: Compromise solutions according to the criteria priorities and L_2 metric. Results of CO_2 emissions

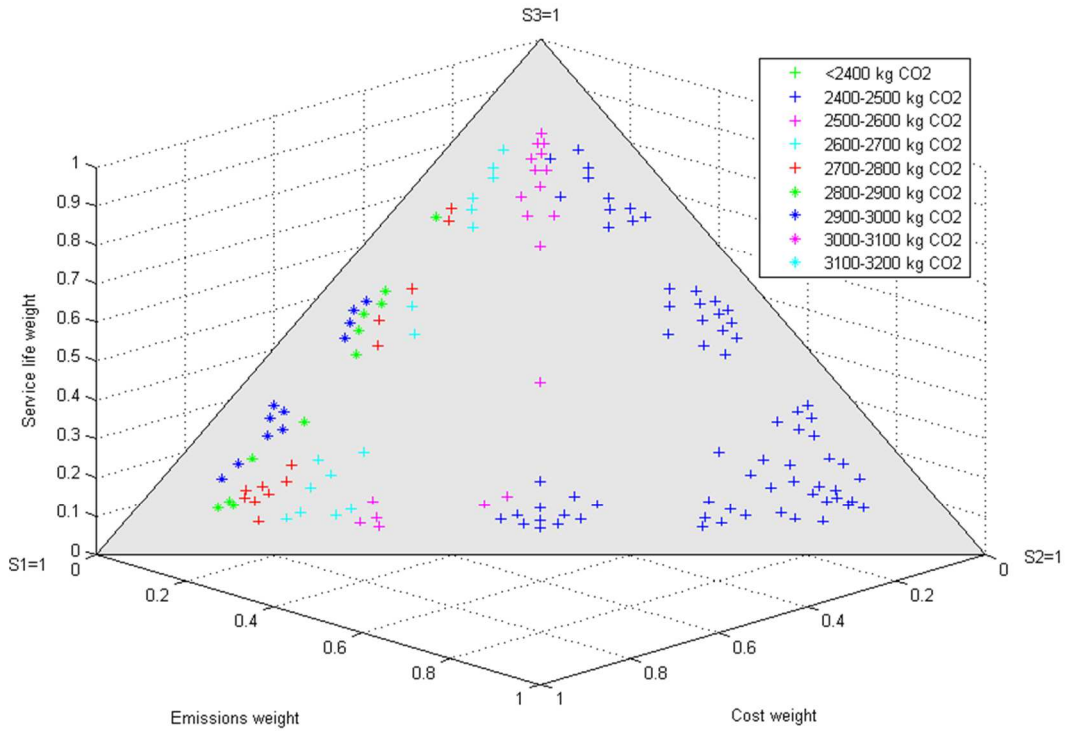

Figure 15: Compromise solutions according to the criteria priorities and L_∞ metric. Results of CO_2 emissions

Figure 16 shows the robustness of the service life when L_1 is used. All solutions had a service life greater than 450 years. However, Figures 17 and 18 show lower values of service life. The percentage of solutions whose service life was greater than 450 years was 76 and 65% for the L_2 and L_∞ metrics, respectively. In general terms, the findings indicate that L_∞ seeks a good balance between criteria with less dependence on weighting, while L_1 has a greater correlation with weights. At the same time, the results show that the service life criterion has a direct relation with sustainability, since long-term structures obtain a good equilibrium between the criteria chosen to achieve this goal.

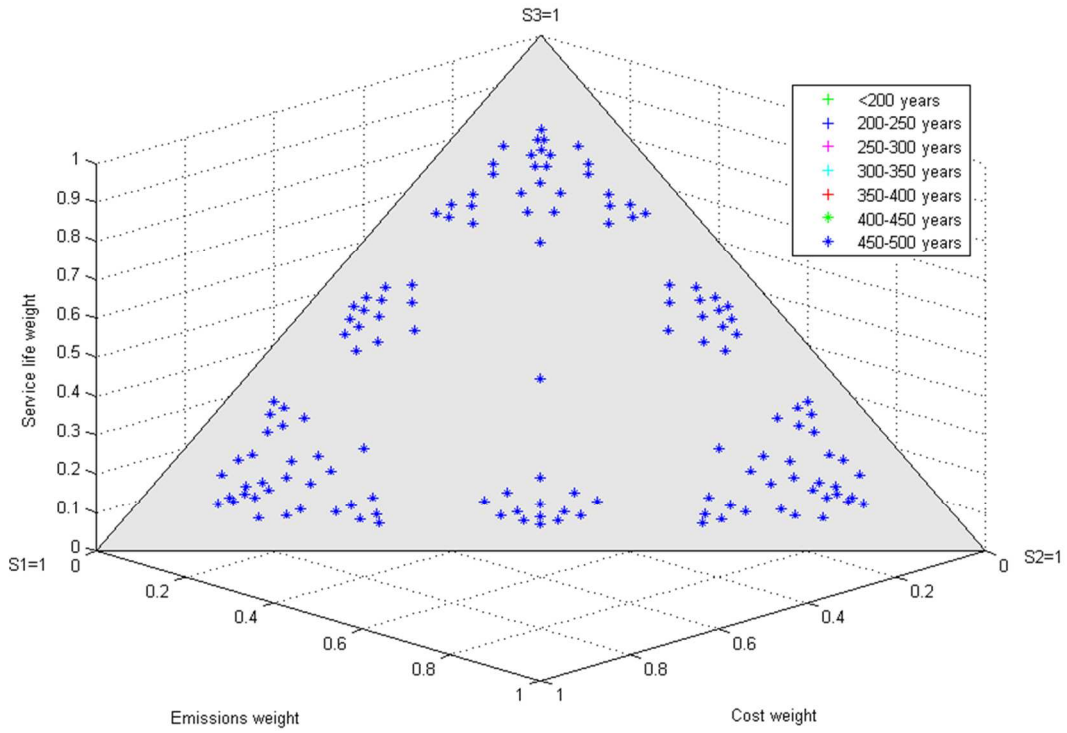

Figure 16: Compromise solutions according to the criteria priorities and L_1 metric. Results of service life

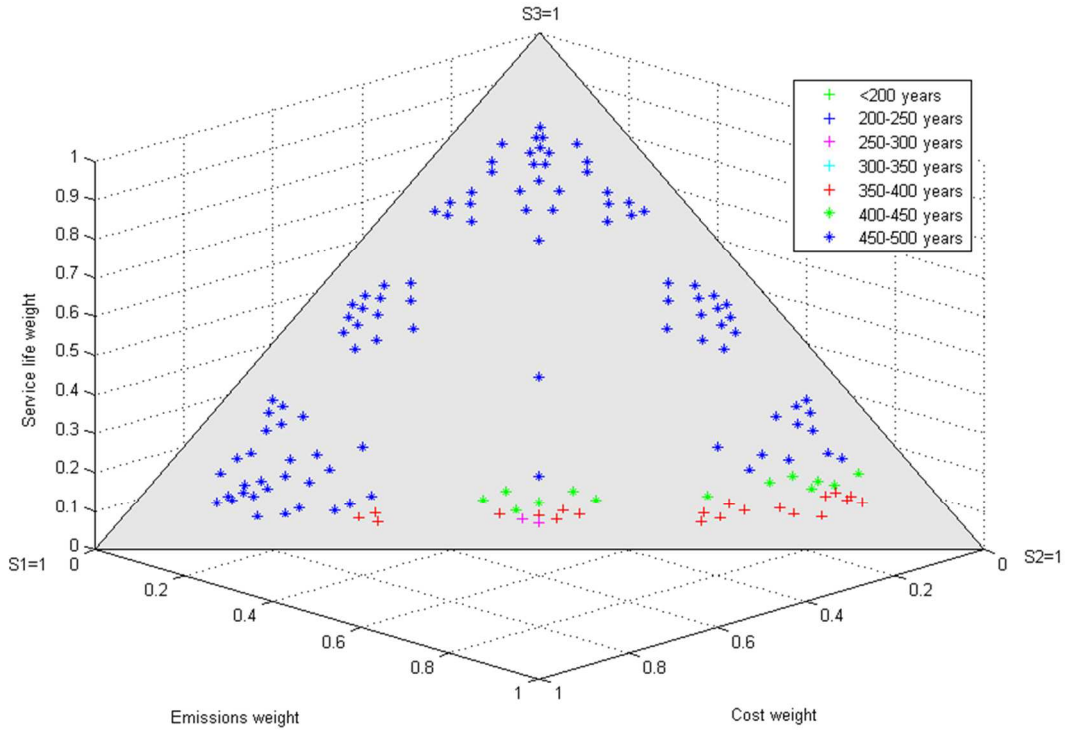

Figure 17: Compromise solutions according to the criteria priorities and L_2 metric. Results of service life

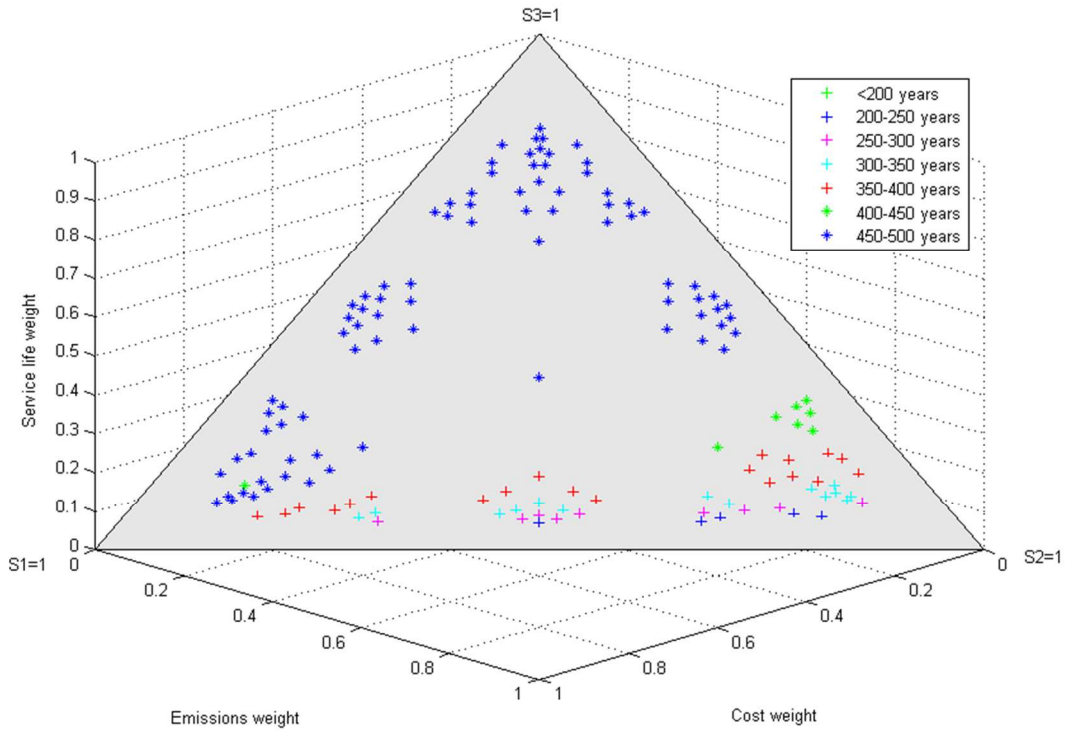

Figure 18: Compromise solutions according to the criteria priorities and L_∞ metric. Results of service life

3.3 Step 3: Analytic Hierarchy Process

The objective of this step is to introduce the DM's preferences for selecting the preferred solution. Expert preferences were provided through pairwise comparison matrices using Saaty´s fundamental scale [20], specified in Table 4. The matrix measures the relative importance of the compared elements. Besides, the consistency of the judgments was verified. Finally, the criteria priorities measured in an absolute scale were obtained with the eigenvector method, since this is the most widely used. For this example, a set of experts provided by consensus the pairwise comparison matrix, which is shown in Table 5. The priorities derived were $w = (w_1, w_2, w_3) = (0.637, 0.105, 0.258)$. The consistency ratio (CR) guaranteed a good consistency as it was lower than 0.1 (CR = 0.037).

Table 6 gives the preferred solutions for each metric. The second and third closest solutions are provided for drawing conclusions regarding concrete strength. Both L_1 and L_2 achieved the same solutions. The concrete strength was 80 MPa for the three solutions. Looking at the criteria, the service life obtained the maximum value of 500 years. Regarding the L_∞ metric, the best solution corresponded to 70 MPa concrete, whereas the second and third solutions used 60 MPa concrete. In this case, the cost was increased while the service life and the emissions were reduced to minimize the distance.

3.4 Step 4. Cognitive approach

Finally, the preferred solutions were compared with the best solution for the minimum cost in a single objective optimization [33]. Table 7 shows that the preferred solutions were about 3 and 4% more expensive. However, the emissions were 7 and 11% lower and the service life was improved by about 233%. Comparing the mean characteristics of the preferred solutions, it is worth noting the reduction in the amount of steel and the increment in depth, concrete strength, and concrete cover. High depth led to an increment in CO_2 capture and therefore an emission reduction. High-strength concrete and greater concrete cover increased the service life. Compared with the other metrics, the Tchebycheff metric preferred the more ecological and less economical solutions. Therefore, this metric selected greater concrete cover and lower concrete strength to achieve a lifetime of 500 years.

4. Conclusions

This paper presents a methodology for generating, analyzing and filtering the Pareto optimal set and selecting the preferred solution for the multi-objective optimization of structural problems. At the same time, the economic and ecological sustainability of a high-strength concrete I-beam is examined. The study proposes costs, CO_2 emissions, and service-life as criteria for attaining a sustainable structural design. In the first step of the methodology, the Pareto optimal set is defined using the multi-objective optimization technique. The comparative analysis of these non-dominated solutions provides a guide to enhancing the sustainability of the structural design. The second step reduces the number of Pareto points using the closest solutions to the ideal, according to the three Minkowsky metrics. These compromise solutions represent 2%, 6% and 15% of the Pareto set, depending on which metric is used: the Manhattan (p = 1), Euclidean (p = 2), or Tchebycheff (p = ∞). The cognitive orientation for the compromise solutions provides the information that promotes learning about the decision-making process. While the Pareto set offered solutions with 30-80 MPa concrete, the reduction to a set of compromise solutions recommended high-strength concrete. Moreover, these solutions imply longer-life structures. The DM's preferences, provided by mean of the judgments of the pairwise comparison matrix, were then used to choose the preferred solutions. These solutions increased service-life by 233% and reduced emissions by 7% and 11%; costs only increased by about 3% and 4%.

Acknowledgments

The Spanish Ministry of Science and Innovation and FEDER founds supported this work through two research projects: “BRIDLIFE” (Ref. BIA2014-56574-R) for the first two authors and “Social Cognocracy Network” (Ref. ECO2011-24181) for the third.

References

[1] E.K. Zavadskas, T. Vilutiene, Z. Turskis, J. Saparauskas, Multi-criteria analysis of Projects’ performance in construction. Archives of Civil and Mechanical Engineering 14(1) (2014) 114-121.

[2] M. Medineckiene, E.K. Zavadskas, F. Bjork, Z. Turskis, Multi-criteria decision-making system for sustainable building assessment/certification. Archives of Civil and Mechanical Engineering 15(1) (2015) 11-18.

[3] A. Altuzarra, P. Gargallo, J.M. Moreno-Jiménez, M. Salvador, Influence, relevance and discordance of criteria in AHP-Global Bayesian prioritization, International Journal of Information Technology & Decision Making 12 (4) (2013) 837–861.

[4] J.M. Moreno-Jiménez, J. Cardeñosa, C. Gallardo, M.A. de la Villa-Moreno, A new e-learning tool for cognitive democracies in the Knowledge Society, Computers in Human Behavior 30 (2014) 409–418.

[5] J.M. Moreno-Jiménez, C. Pérez-Espés, M. Velázquez, e-Cognocracy and the design of public policies, Government Information Quarterly 31 (1) (2014) 185–194.

[6] T.W. Liao, P.J. Egbelu, B.R. Sarker, S.S. Leu, Metaheuristics for project and construction management – A state-of-the-art review, Automation in Construction 20 (5) (2011) 491–505.

[7] C. Chiu, Y. Lin, Multi-objective decision-making supporting system of maintenance strategies for deteriorating reinforced concrete buildings, Automation in Construction 39 (2014) 15–31.

[8] I. Paya, V. Yepes, F. González-Vidosa, A. Hospitaler, Multiobjective optimization of reinforced concrete building frames by simulated annealing, Computer-Aided Civil and Infrastructure Engineering 23 (8) (2008) 596–610.

[9] F. Martinez-Martin, F. Gonzalez-Vidosa, A. Hospitaler, V. Yepes, Multi-objective optimization design of bridge piers with hybrid heuristic algorithms, Journal of Zhejiang University SCIENCE A 13 (6) (2012) 420–432.

[10] D.J.M. Flower, J.G. Sanjayan, Greenhouse gas emissions due to concrete manufacture, The International Journal of Life Cycle Assessment 12 (5) (2007) 282–288.

[11] F. Collins, Inclusion of carbonation during the life cycle of built and recycled concrete: influence on their carbon footprint, The International Journal of Life Cycle Assessment 15 (6) (2010) 549–556.

[12] T. García-Segura, V. Yepes, J. Alcalá, Life-cycle greenhouse gas emissions of blended cement concrete including carbonation and durability, The International Journal of Life Cycle Assessment 19 (1) (2014) 3–12.

[13] B. J. Hancock, C.A. Mattson, The smart normal constraint method for directly generating a smart Pareto set, Structural and Multidisciplinary Optimization 48 (4) (2013) 763–775.

[14] L. Rachmawati, D. Srinivasan, Multiobjective evolutionary algorithm with controllable focus on the knees of the Pareto front, IEEE Transactions on Evolutionary Computation 13 (4) (2009) 810 – 824.

[15] S. Saha, S. Bandyopadhyay, A new multiobjective clustering technique based on the concepts of stability and symmetry, Knowledge and Information Systems 23 (1) (2010) 1-27.

[16] C.A. Mattson, A.A. Mullur, A. Messac, Smart Pareto filter: obtaining a minimal representation of multiobjective design space, Engineering Optimization 36 (6) (2004) 721–740.

[17] P.Ashoka Varthanan, N. Murugan, G.M Kumar, An AHP based heuristic DPSO algorithm for generating multi criteria production–distribution plan, Journal of Manufacturing Systems 32(4) (2013) 632-647.

[18] V. Muerza, D. De Arcocha, E. Larrodé, J.M. Moreno-Jiménez, The multicriteria selection of products in technological diversification strategies: An application to the Spanish automotive industry based on AHP, Production Planning and Control. The Management of Operations 25 (8) (2014) 715-728.

[19] A. Altuzarra, J.M. Moreno-Jiménez, M. Salvador, Consensus Building in AHP-Group Decision Making: A Bayesian approach, Operations Research 58 (6) (2010) 1755-1773.

[20]T.L. Saaty, The Analytic Hierarchy Process, RWS Publication, Pittsburgh, 1990.

[21] T. García-Segura, V. Yepes, J.V. Martí, J. Alcalá, Optimization of concrete I-beams using a new hybrid glowworm swarm algorithm, Latin American Journal of Solids and Structures 11 (7) (2014) 1190–1205.

[22] B. Lagerblad, Carbon Dioxide Uptake during Concrete Life-Cycle: State of the Art, Swedish Cement and Concrete Research Institute, Stockholm, 2005.

[23] SendeCO_2 (2014), Available at: http://www.sendeco2.com (accessed November 2014).

[24] Catalonia Institute of Construction Technology, BEDEC PR/PCT ITEC Materials Database (2014), Available at: http://www.itec.cat (accessed November 2014)

[25] European Federation of Concrete Admixtures Associations, Environmental Product Declaration (EPD) for Normal Plasticising Admixtures (2006), Available at: http://www.efca.info/downloads/324%20ETG%20Plasticiser%20EPD.pdf (accessed November 2014).

[26] M. Fomento, Code on Structural Concrete EHE-08, Ministerio de Fomento, Madrid, Spain, 2008. (in Spanish).

[27] K. Tuutti, Corrosion of Steel in Concrete, CBI Forskning Research Report, Cement and Concrete Research Institute, Stockholm, Sweden, 1982.

[28] P. Serafini, Simulated annealing for multiple objective optimization problems, Proc. 10th Int. Conf. Multiple Criteria Decision Making, Taipei, 1992, pp. 87–96.

[29] N. Metropolis, A. W. Rosenbluth, M. N. Rosenbluth, A. H. Teller, E. Teller, Equation of state calculations by fast computing machines, The Journal of Chemical Physics 21 (1953) 1087.

[30] R.J. Glauber, Time-dependent statistics of the Ising model, Journal of Mathematical Physics 4 (2) (1963) 294.

[31] J. Medina, Estimation of incident and reflected waves using simulated annealing, Journal of Waterway, Port, Coastal, and Ocean Engineering 127 (4) (2001) 213–221.

[32] I. Payá-Zaforteza, V. Yepes, F. González-Vidosa, A. Hospitaler, On the Weibull cost estimation of building frames designed by simulated annealing, Meccanica 45 (5) (2010) 693-704.

[33] T. García-Segura, V. Yepes, J. Alcalá, Sustainable design using multiobjective optimization of high-strength concrete I-beams, The 2014 International Conference on High Performance and Optimum Design of Structures and Materials HPSM/OPTI 2014, 9–11 June, Ostend, Belgium, 2014.

APPENDIX: Notation

The following symbols are used in this paper:

A (m^2) = exposed surface area of concrete;

b_{fs} (m) = width of the top flange;

b_{fi} (m) = width of the bottom flange;

C (€) = economic cost;

c (kg/m^3)= quantity of Portland cement per cubic meter of concrete;

CaO = CaO content in Portland cement;

C_{CO2} (kg) = CO_2 captured;

CR = consistency ratio;

E (kg) = CO_2 emissions;

e_i (kg CO_2/m^3, kg CO_2/m^2, kg CO_2/kg, kg CO_2/m, kg CO_2/tCO_2) = unit emissions;

$f_{i,t}$ (€, kg CO_2, years)= objective functions;

f_{ck} (MPa)= concrete compressive strength;

g_i = constraints;

h (m) = depth;

Ic = indices set of structural costs;

Ie = indices set of structural emissions;

I_G = indices set of structural constraints;

k ($mm/year^{0.5}$) = carbonation rate coefficient;

L_1 = distance to the ideal using Manhattan metric;

L_2 = distance to the ideal using Euclidean metric;

L_3 = distance to the ideal using Tchebycheff metric;

M= chemical molar fraction CO_2/CaO;

m_i (m^3, m^2, kg, m, tCO_2) =measurements;

M_d (KN.m) = acting bending resultant

n_i = number of bars;

p = distance norm

pc = proportion of calcium oxide that can be carbonated;

p_i (€/m^3, €/m^2, €/kg, €/m, €/tCO_2) = unit prices;

r (mm) = concrete cover;

S_i= simplex vertices;

SL (year) = service life;

T (€, kg CO_2, years) = temperature;

t_{fi} (m) = thickness of the bottom flange;

t_{fs} (m) = thickness of the top flange;

t_w (m) = web thickness;

v_c (μm/year) = corrosion speed;

z_j (€, kg CO_2, years) = criteria;

w_j = weights of importance criteria;

α = coefficient of cooling;

$Ø_i$ (mm) = the diameter of bars;

$Ø_r$ (mm) = most restrictive variable for the bar diameter;

λ_j ($€^{-1}$, kg CO_2^{-1}, $years^{-1}$) = normalized weights of importance criteria;

List of Tables and Figures

Table 1: Unit prices and CO_2 emissions considered in the RC I-beam

	Construction units	Cost (euros)	CO_2 emissions (kg)
m^3	Concrete HA-30 in beams	97.67	259.61
m^3	Concrete HA-35 in beams	102.37	277.61
m^3	Concrete HA-40 in beams	107.07	295.61
m^3	Concrete HA-45 in beams	111.77	313.61
m^3	Concrete HA-50 in beams	116.47	331.61
m^3	Concrete HA-55 in beams	121.17	349.61
m^3	Concrete HA-60 in beams	125.87	367.61
m^3	Concrete HA-70 in beams	135.27	403.61
m^3	Concrete HA-80 in beams	144.67	439.61
m^3	Concrete HA-90 in beams	154.07	475.61
m^3	Concrete HA-100 in beams	163.47	511.61
kg	Steel B-500-SD	1.24	3.03
m^2	Formwork in beams	33.81	2.08
m	Beam placing	16.86	39.43
t CO_2	CO_2 cost	6.00	

Table 2. Mix design properties and cement content

Unit	**k (mm/year$^{0.5}$)**	**c (kg/m^3)**
Concrete HA-30 in beams	3.71	280
Concrete HA-35 in beams	3.01	300
Concrete HA-40 in beams	2.50	320
Concrete HA-45 in beams	2.11	350
Concrete HA-50 in beams	1.81	400
Concrete HA-55 in beams	1.57	457
Concrete HA-60 in beams	1.38	485
Concrete HA-70 in beams	1.09	493
Concrete HA-80 in beams	0.89	497
Concrete HA-90 in beams	0.74	517
Concrete HA-100 in beams	0.63	545

Table 3. Summary of the best algorithms results

Criterion	Variables changed in each iteration (%)	Restart criterion (number of chains)	Markov chain	Cooling coefficient	Cost (€)	Emission (kg CO_2)	Service life (years)
Metropolis	20	5	30,000	0.95	2880.435	2305.574	500
Glauber	20	5	10,000	0.95	2872.351	2258.911	500

Table 4. Saaty's fundamental scale [17]

Numerical scale	Verbal scale	Explanation
1	Same importance	The two elements make a similar contribution to the criterion.
3	One item moderately more important than another	Judgment and earlier experience favor one element over another.
5	One item significantly more important than another	Judgment and earlier experience strongly favor one element over another.
7	One item much more important than another	One element dominates strongly. Its domination is proven in practice.
9	One item very much more important than another.	One element dominates the other with the greatest order or magnitude possible

Table 5. Pairwise comparison matrix

	Cost	Emission	Service life	W
Cost	1	5	3	0.637
Emission	1/5	1	1/3	0.105
Service life	1/3	3	1	0.258

CR = 3.7%

Table 6. Preferred solutions for the L_p metrics with p = 1, 2, ∞.

		Weights	0.637	0.105	0.258	
Metric	**Solution**	**Distance**	**Cost (€)**	**Emission (kg CO_2)**	**Service life (years)**	**f_{ck} (MPa)**
L_1	143	0.0338	2,929	2,973	500	80
	144	0.0338	2,930	2,971	500	80
	263	0.0339	2,931	2,969	500	80
L_2	143	0.0253	2,929	2,973	500	80
	144	0.0253	2,930	2,971	500	80
	263	0.0253	2,931	2,969	500	80
L_∞	291	0.0188	2,969	2,847	500	70
	244	0.0190	2,965	2,851	495	60
	73	0.0195	2,954	2,731	462	60

Table 7. Mean characteristics for the cost-optimized and preferred solutions

	Cost-optimized (single objective optimization)	**Preferred solution L_1 and L_2 metric (multi-objective optimization)**	**Preferred solution L_∞ metric (multi-objective optimization)**
***h* (mm)**	1250	1400	1500
b_{fs} (mm)	250	350	300
b_{fi} (mm)	200	200	200
t_{fs} (mm)	170	100	80
t_{fi} (mm)	130	130	130
t_w (mm)	80	80	90
***r* (mm)**	17	19	21
f_{ck} (MPa)	45	80	70
Steel (kg)	671.85	494.31	472.06
Concrete (m^3)	2.08	2.26	2.43
CO_2 capture(kg CO_2)	169.17	213.82	265.95
Cost (€)	2854.29	2929.31	2969.40
Emission (kg CO_2)	3204.17	2972.94	2847.00
Service life (years)	150	500	500

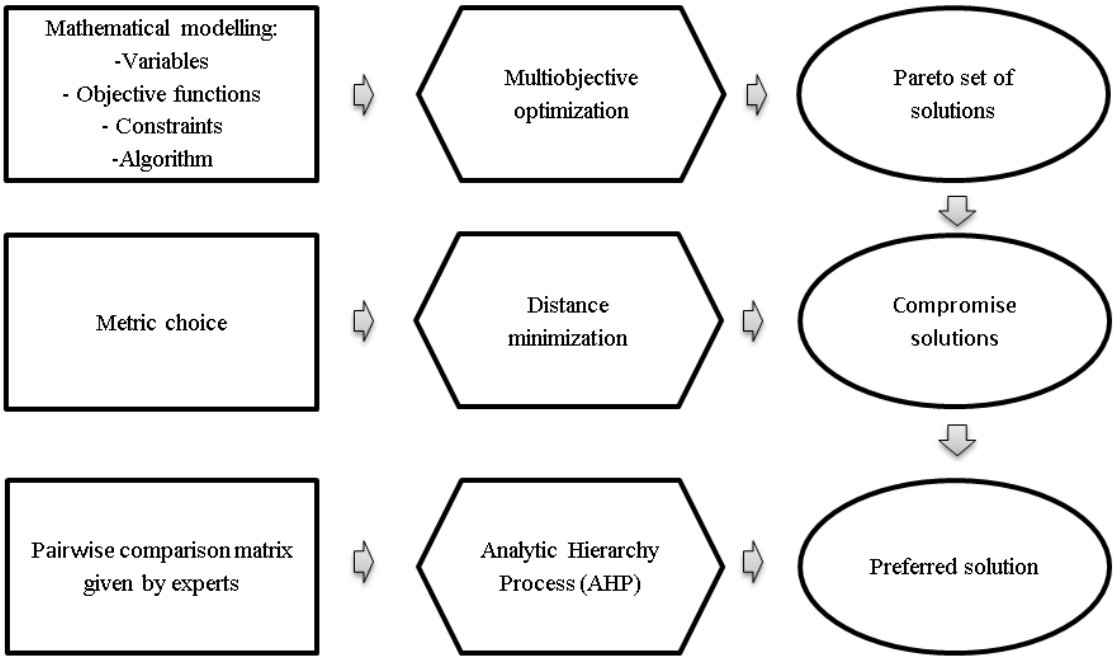

Figure 1. $[PS]^2$-methodology

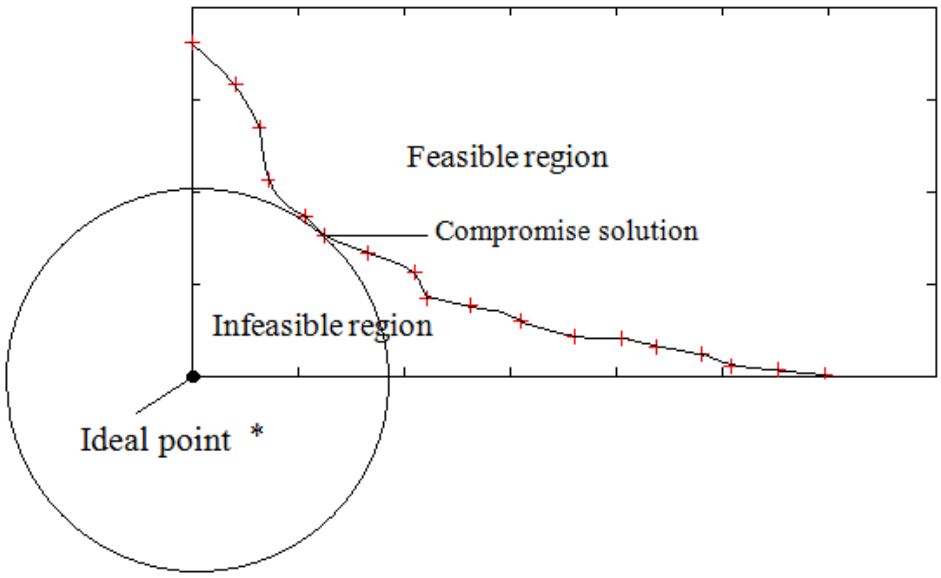

Figure 2. Compromise solution using the L_2 norm

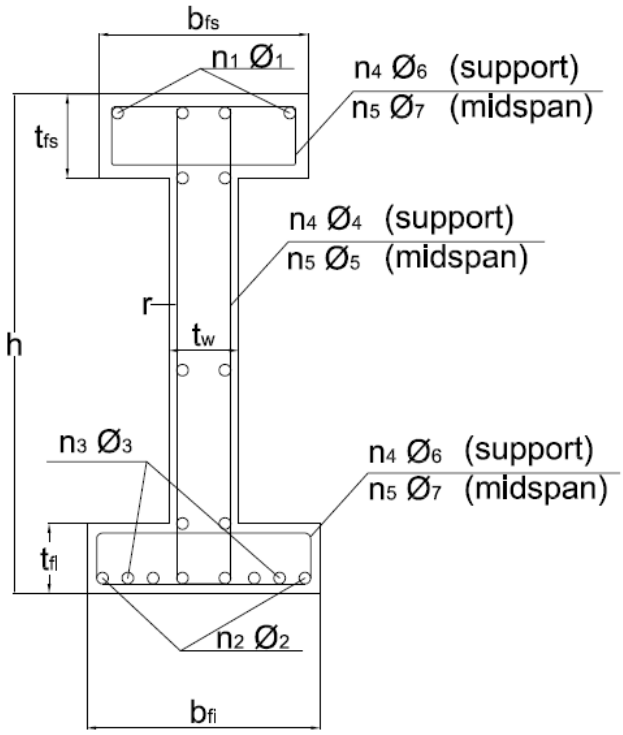

Figure 3: Design variables of the reinforced concrete I-beam

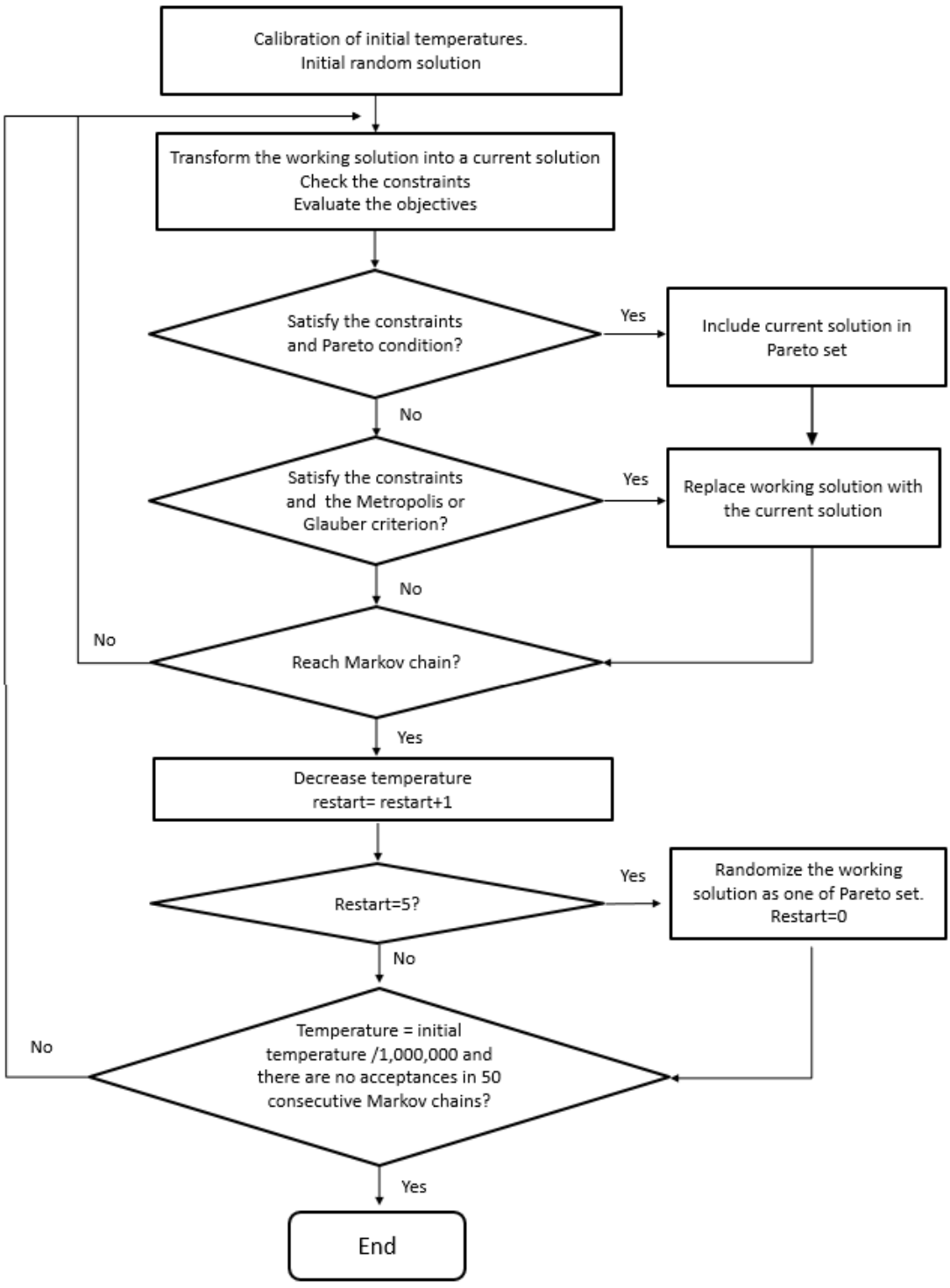

Figure 4: Flowchart of the MOSA process

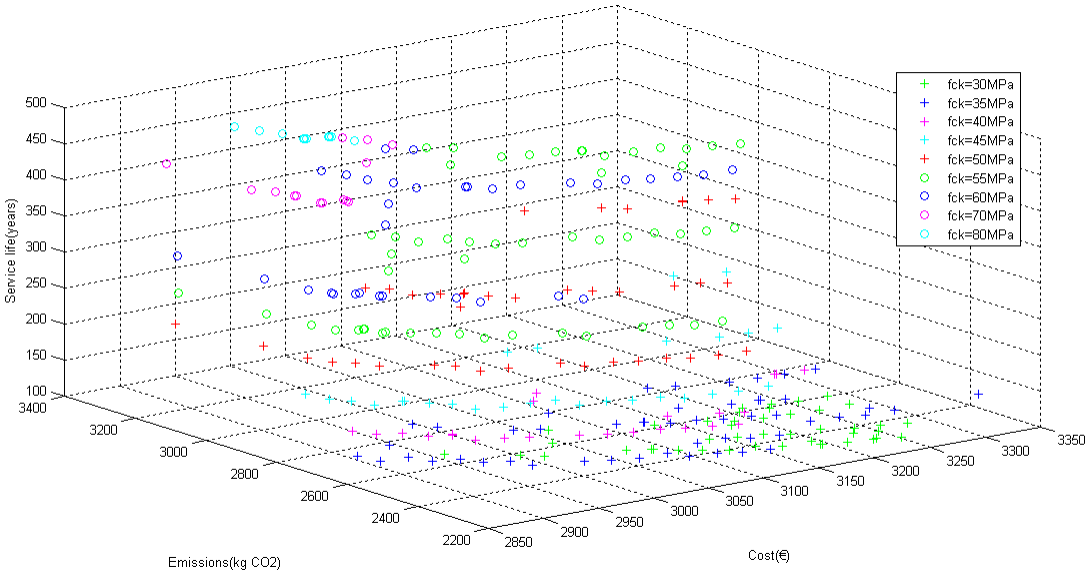

Figure 5: Pareto set of solutions

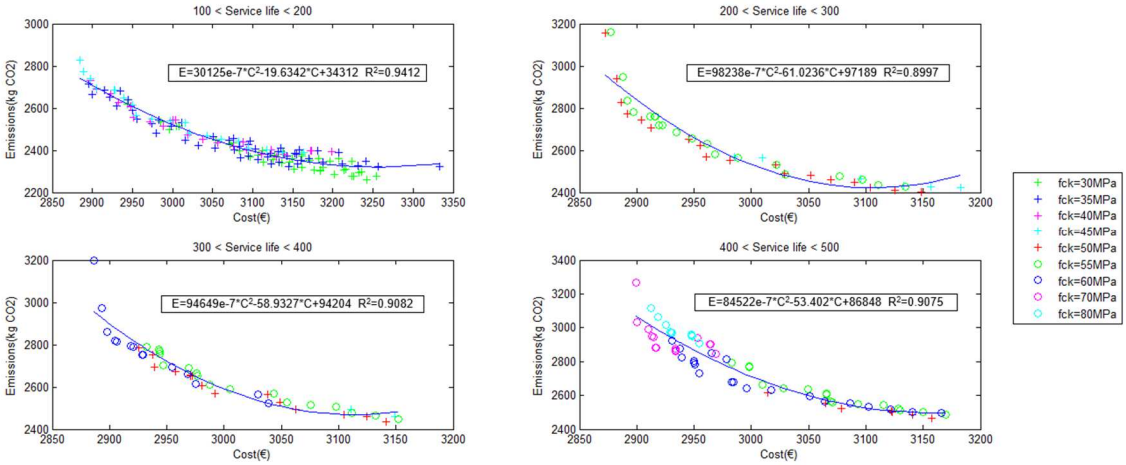

Figure 6: Pareto set according to service life range

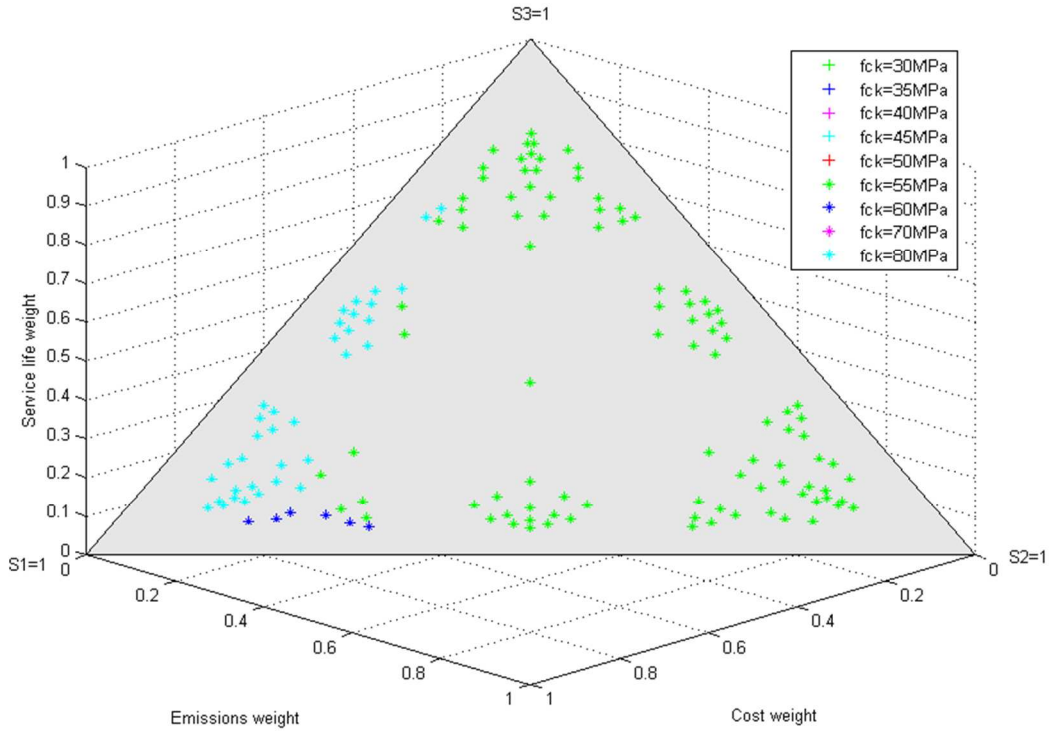

Figure 7: Compromise solutions according to the criteria priorities and L_1 metric. Results of concrete strength

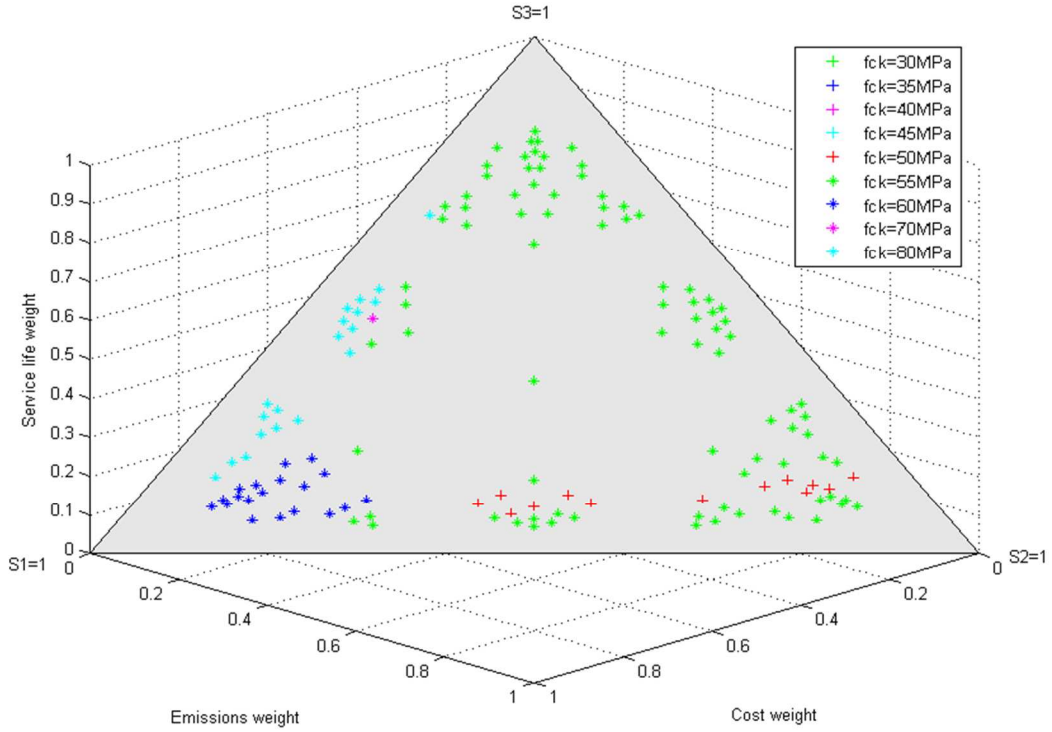

Figure 8: Compromise solutions according to the criteria priorities and L_2 metric. Results of concrete strength

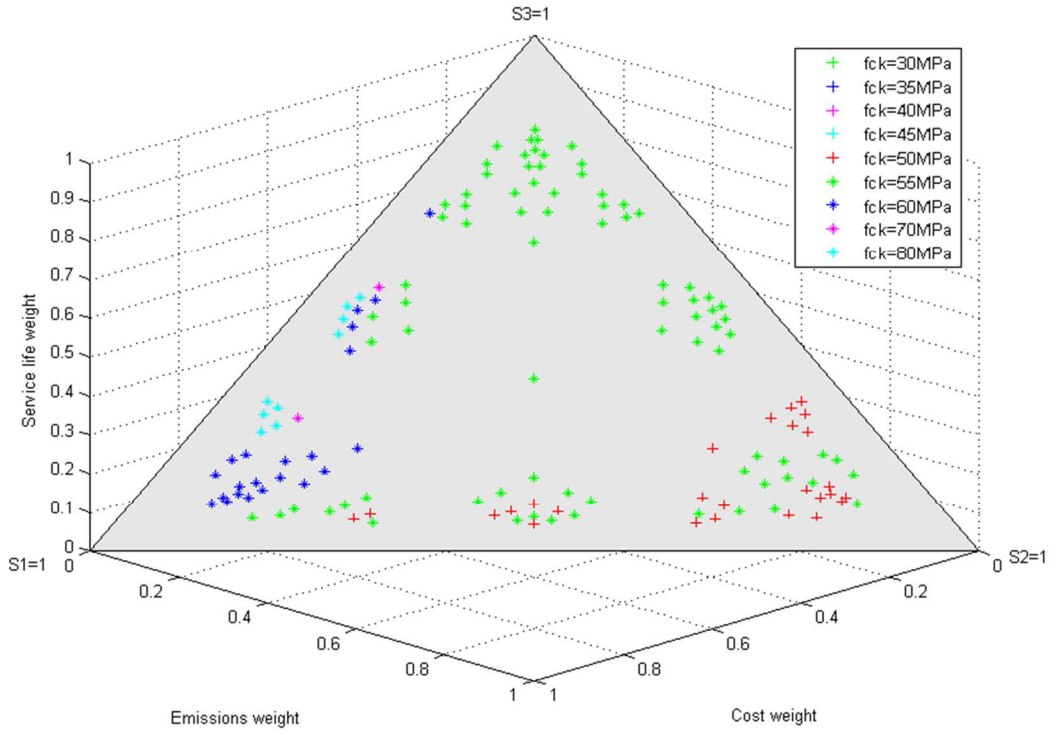

Figure 9: Compromise solutions according to the criteria priorities and L_∞ metric. Results of concrete strength

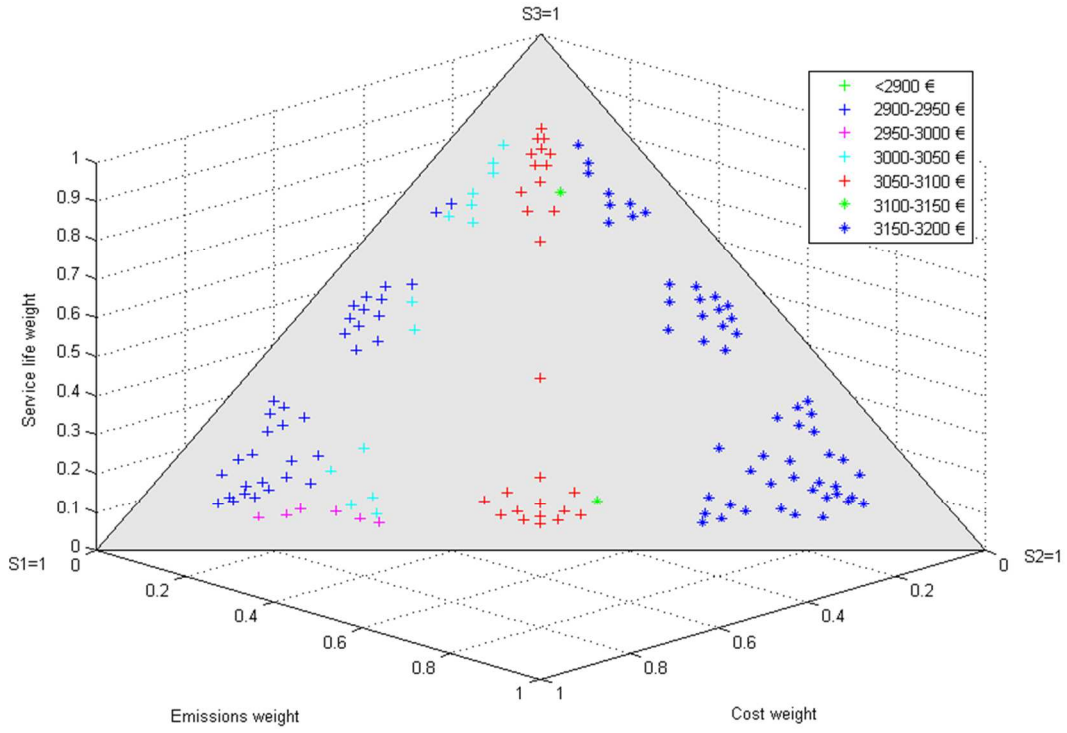

Figure 10: Compromise solutions according to the criteria priorities and L_1 metric. Results of cost

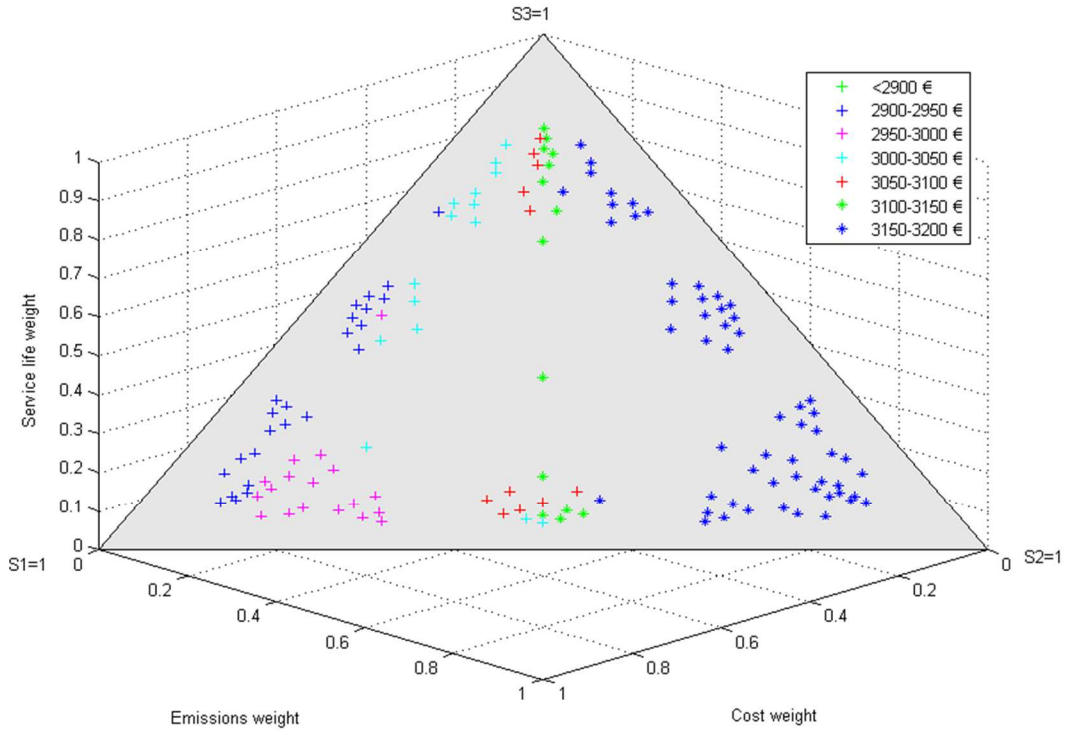

Figure 11: Compromise solutions according to the criteria priorities and L_2 metric. Results of cost

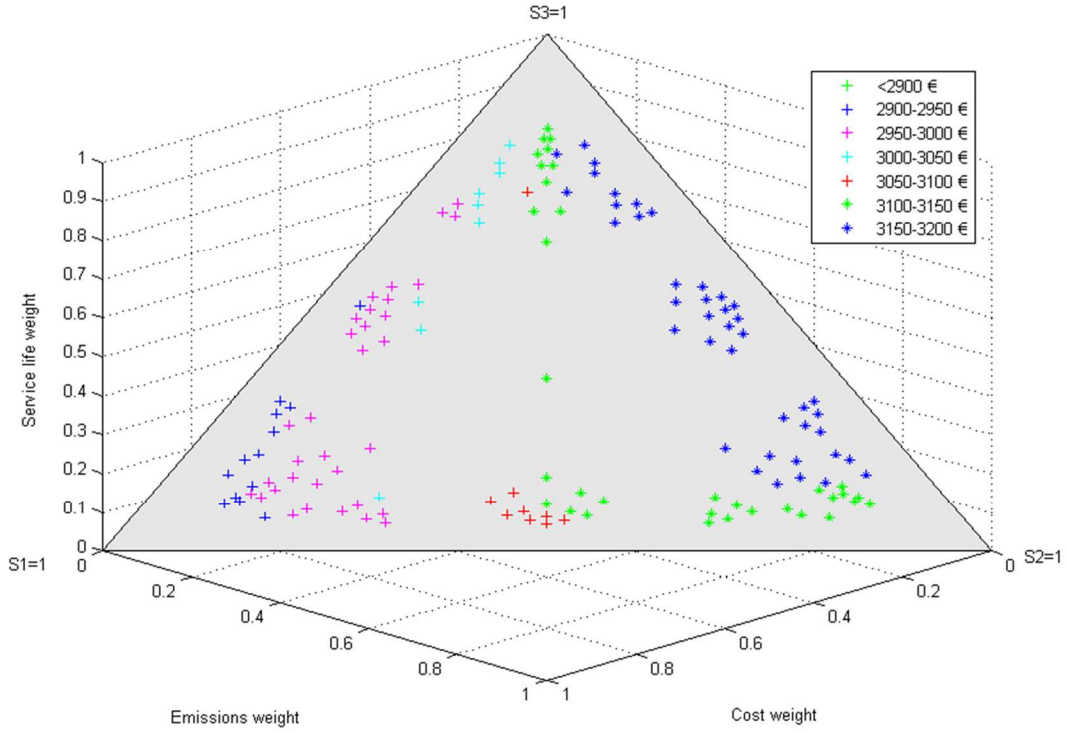

Figure 12: Compromise solutions according to the criteria priorities and L_∞ metric. Results of cost

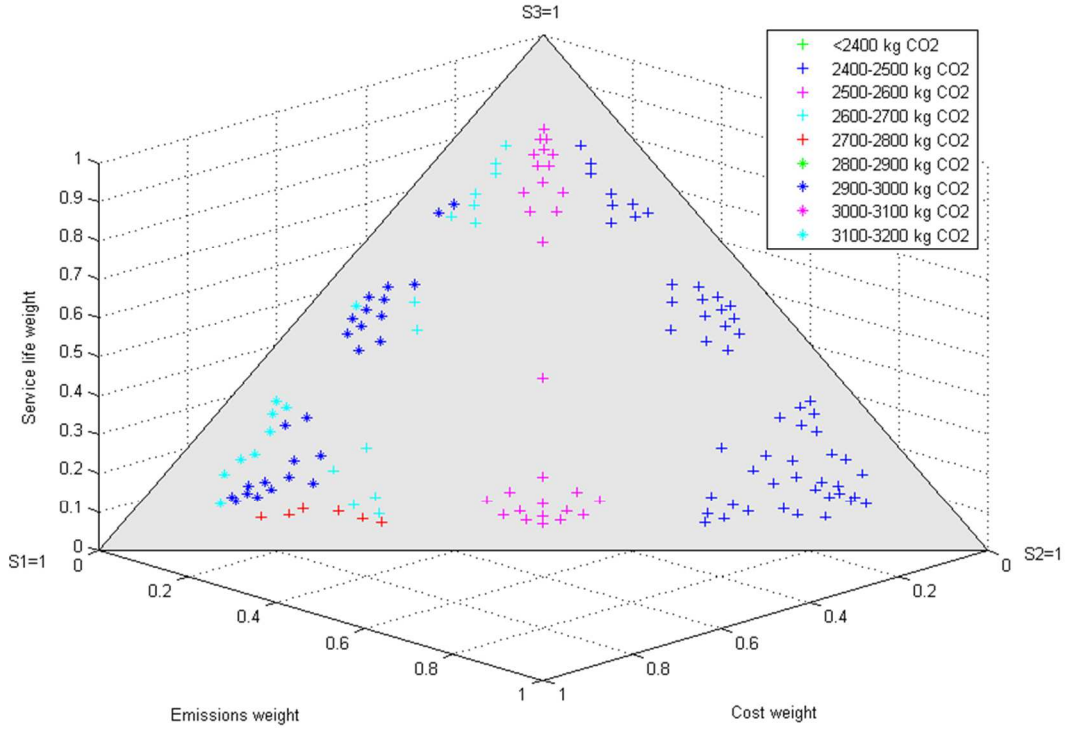

Figure 13: Compromise solutions according to the criteria priorities and L_1 metric. Results of CO_2 emissions

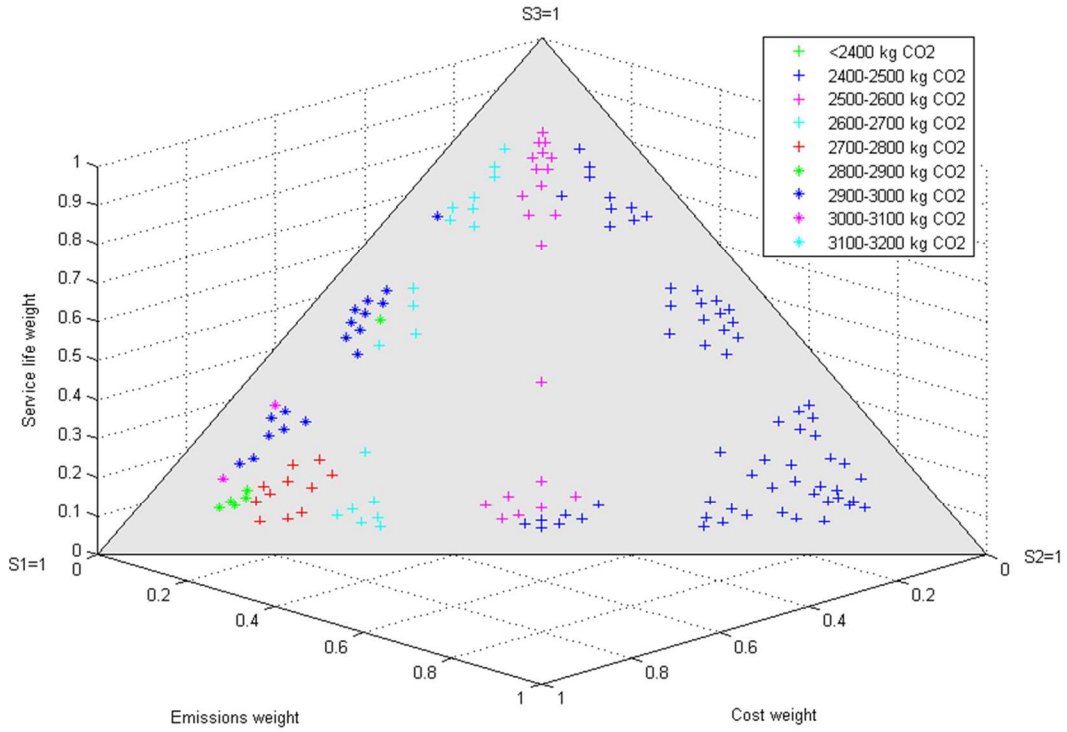

Figure 14: Compromise solutions according to the criteria priorities and L_2 metric. Results of CO_2 emissions

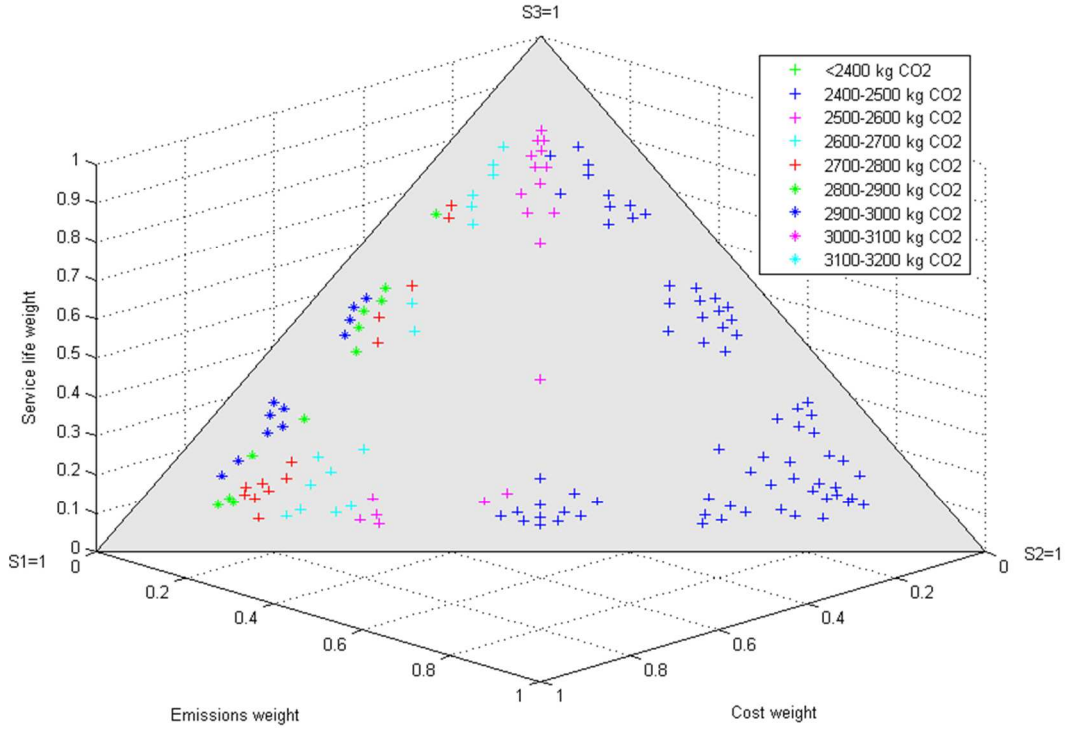

Figure 15: Compromise solutions according to the criteria priorities and L_∞ metric. Results of CO_2 emissions

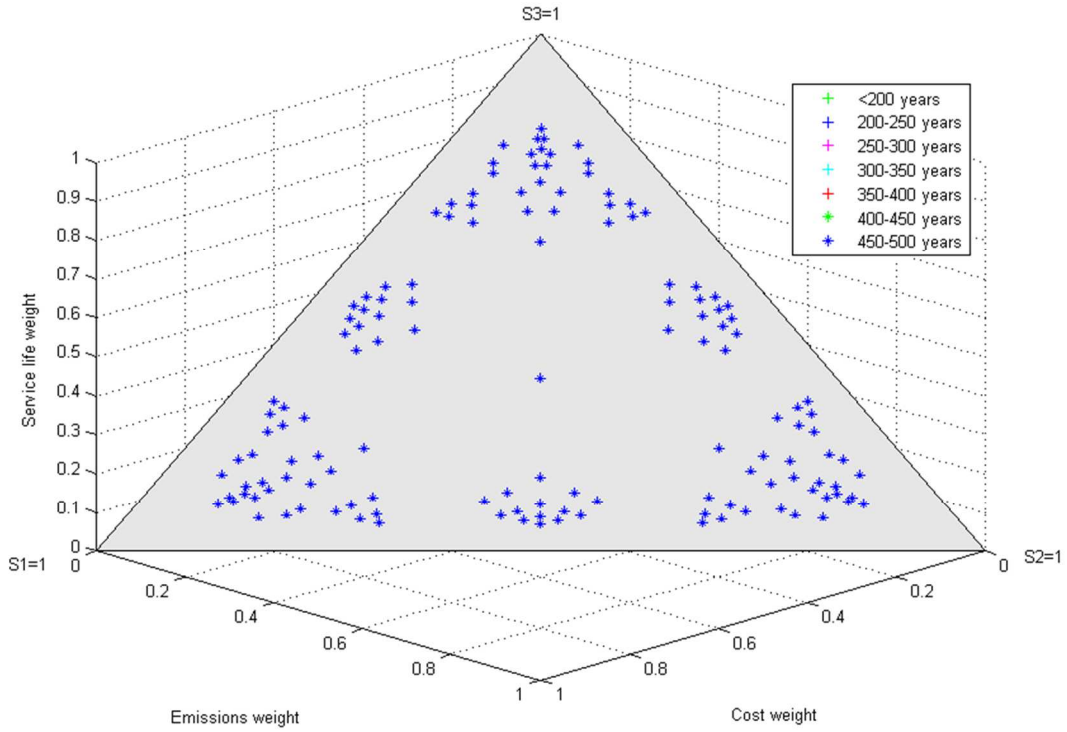

Figure 16: Compromise solutions according to the criteria priorities and L_1 metric. Results of service life

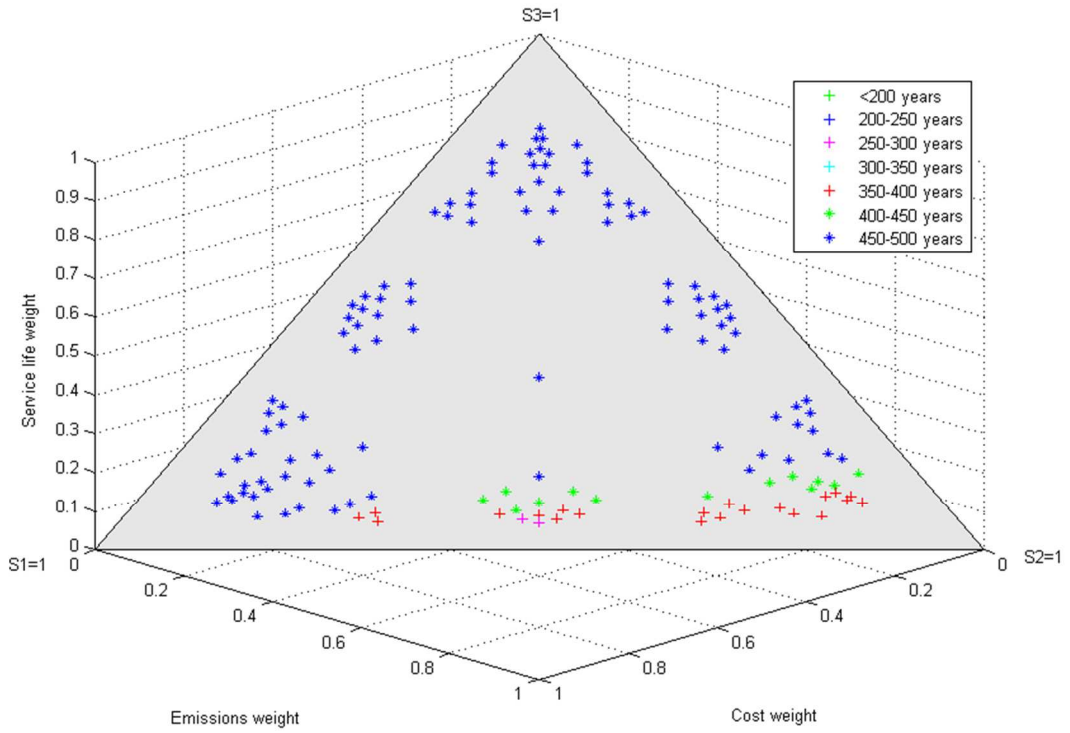

Figure 17: Compromise solutions according to the criteria priorities and L_2 metric. Results of service life

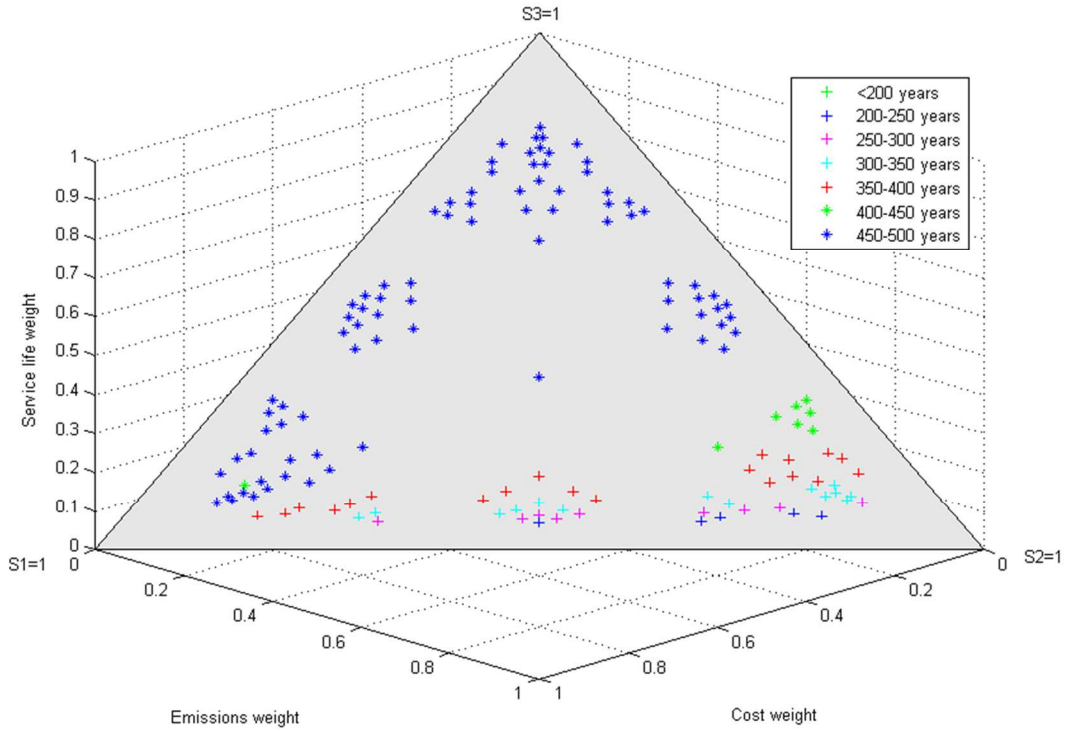

Figure 18: Compromise solutions according to the criteria priorities and L_∞ metric. Results of service life